WAVEFORM SHAPING FOR DIRECTLY MODULATED LASER DIODE

WAVEFORM SHAPING FOR DIRECTLY MODULATED LASER DIODE

BY

YI LAN, B.SC.

A Thesis

Submitted to the School of Graduate Studies

in Partial Fulfilment of the Requirements

for the Degree

Master of Applied Science

McMaster University

MASTER OF APPLIED SCIENCE (2008) McMaster University

Electrical and Computer Engineering Hamilton, Ontario

TITLE: Waveform Shaping for Directly Modulated Laser Diodes

AUTHOR: Yi Lan, B.Sc. (HoHai University)

SUPERVISOR: Professor Weiping Huang

NUMBER OF PAGES: x, 68

Abstract

The objective of this thesis is to study the dynamic properties of laser diodes and the compensation for the nonlinearities of laser diodes based on the theory of Volterra series.

In the first part of this thesis, an analytical expression in Volterra series is discussed to depict the nonlinear distortion of laser diodes up to the third order. The simulation results of this analytical method show that Volterra series model improves the accuracy of the description of the nonlinearity of laser diodes in comparison with small-signal analysis model.

In the second part, the p^{th}-order inverse theory is introduced to compensate the lasers' nonlinear distortion. The compensation scheme is constructed and the simulation of the system is conducted in this thesis. The result shows that the laser nonlinear distortion can be compensated by using this technique.

Acknowledgement

I would like to express my gratitude to all those who gave me the possibility to complete this thesis.

At the very first, I'm honored to express my deepest gratitude to my supervisor, Prof. Weiping Huang, with whose guidance I could have worked out this thesis. His suggestion, encouragement and patience are greatly appreciated.

Sincere thanks to Dr. Li and Dr. Chen, for their reading and suggesting about my thesis. Thanks to the faculty and administrative & technical staff of Electrical and Computer Engineering, for their support of my study.

Also thanks to my colleagues and friends, Lanxin Deng, Jianwei Mu, Yanping Xi, lin Han, Yu Li, who give me great suggestions and help in my study and life.

At last but not least, I would like to dedicate this thesis to my parents, Yushi Lan and Xiaomei Zhang. And give my special thanks to Min Huang. This work can not be finished without all their patient love and support.

Contents

List of Figures

List of Tables

Chapter 1
Introduction

1.1 Background and Motivation

Semiconductor lasers are widely used as sources in many optic lightwave transmission systems. The direct modulation technique of the laser diode is attractive because of its simplicity. The output optical power of a laser is an analog modulation waveform when the laser is modulated above threshold. Under high-speed modulation, the nonlinear distortions generated by the laser diodes become a main limiting factor of the overall system performance. Therefore, there is a need to model the nonlinearity characteristics of the laser diode to an adequate accuracy. Several techniques has been proposed to suppress or compensation the nonlinear distortion of the laser diode. Illing and Kennel [17] demonstrate a technique that using a continuous shaped drive current for the suppression of relaxation oscillations. They derived a differential equation with respect to the driving current as a function of the output wave form.

Volterra series gains our interest because it is a powerful analytical method to model a wide class of nonlinear systems with memory. It predicts adequately accurate level of the nonlinear distortion generated by laser diodes. Salgado and O'Reilly [2] presented a frequency domain analytic study of laser nonlinear distortion based on the Volterra series up to third order. Hassine and Toffano [4] derived analytical output expressions for any arbitrary input waveforms based on Volterra functional series to the second order. The Volterra series provides a more general analysis framework in the distortions caused by nonlinearity and has its own advantage in the degree of accuracy. In the thesis, the Volterra model is constructed in which the nonlinear transfer functions of different orders are derived following the method described by Bussgang, Ehrman, and Graham [8] and Salgado and O'Reilly [2]. In the communication systems, it is necessary to develop a scheme to compensate for the relaxation oscillations of the laser diode to enhance the performance of the system. Several methods have been proposed for equalizing Volterra systems such as the p^{th}-order inverse theory [3], fixed point approach [18], and the root method [19]. In this thesis, the compensation scheme based on the principles of the p^{th}-order inverse is applied to compensate the nonlinear distortions.

1.2 Organization of Thesis

In chapter 2, normalized rate equation formulations are derived and used for the analysis of laser diode dynamics in the thesis. Further, the modulation responses of the laser diodes are examined in detail. At last, a numerical model based on finite difference method is established to obtain 'exact' solutions of the rate equations compared with the analytical solution of the rate equations and used as a benchmark for comparisons with approximate analytical solutions.

In chapter 3, we linearized the rate equations and use the small signal model to simulate the modulation response of the laser diode. It is shown that the small signal model validate only if the amplitude of modulated current is much smaller than the biased current.

In chapter 4, a nonlinear Volterra series is introduced to analyze the large signal response of the laser diode. In comparison with the small signal model, the Volterra series model is a more general model which can describe the nonlinear system.

In chapter 5, a p^{th}-order inverse theory of a nonlinear system is discussed and applied to compensate the nonlinearities of the laser diode.

1.3 Contribution

The main contribution of the thesis is as follows:

1. A Volterra model based on the single-mode rate equations is presented to simulate the dynamical nonlinearity of a directly modulated laser diode response to a modulated rectangular pulse bias above threshold. The second-order and third-order nonlinear distortions are discussed in the time domain.
2. A compensation scheme based on the p^{th}-order inverse theory is

developed to cancel nonlinear distortion in the output of the directed modulated laser diode.

Chapter 2
Rate Equations for Laser Diode

2.1 Review of Rate Equations for Laser Diode

The starting point to analyze the dynamic behavior of laser diode is the single-mode rate equations. The single-mode rate equations including the effect of gain compression term can be expressed as the following forms [5]:

$$\frac{dN(t)}{dt}=\frac{I(t)}{qV_{act}}-\frac{N(t)}{\tau_n}-g_0(N(t)-N_{tr})(1-\varepsilon S(t))S(t) \qquad (2.1.1)$$

$$\frac{dS(t)}{dt}=\Gamma g_0(N(t)-N_{tr})(1-\varepsilon S(t))S(t)-\frac{S(t)}{\tau_s}+\Gamma\beta\frac{N(t)}{\tau_n} \qquad (2.1.2)$$

where $N(t)$ is the electron density, $S(t)$ is the photon density, $I(t)$ is the current injected into the active region, Γ is the optical confinement factor given by the ratio of the active region volume and the total model volume, N_{tr} is the electron density for transparency, V_{act} is the volume of active region, τ_n is the electron lifetime, τ_s is the photon lifetime, g_0 is the gain slop constant, ε is the gain saturation coefficient, β is the fraction of spontaneous emission coupled into the lasing mode, and q is the electronic charge.

The output optical power generated by the laser diode is [20]:

$$P(t)=\frac{S(t)V_{act}\eta h\nu}{2\Gamma\tau_s} \qquad (2.1.3)$$

where η is the external quantum efficiency of the laser is, h is Planck's constant, and υ is the optical frequency.

The threshold current is given by [20]:

$$I_{th} = \frac{qV_{act}}{\tau_n}(N_{tr} + \frac{1}{g_0\tau_s}) \tag{2.1.4}$$

Table 2.1 Parameter Values from DFB laser

parameter	Value	unit
q	1.602×10^{-19}	C
V_{act}	0.45×10^{-16}	m^3
β	1.0×10^{-4}	
Γ	0.25	
ε	2.5×10^{-23}	m^3
g_0	2.9×10^{-12}	$s^{-1}m^3$
N_{tr}	10^{24}	m^{-3}
τ_n	1.0×10^{-9}	s
τ_s	1.0×10^{-12}	s

2.2 Normalized Rate Equations

The various quantities in the rate equations (2.1.1) and (2.1.2) are normalized as follows [1]:

$$t' = \frac{t}{\tau_n},\ N'(t) = g_0\tau_s N(t),\ S'(t) = g_0\tau_n S(t),\ I'(t) = \frac{g_0\tau_n\tau_s}{qV_{act}} I(t),\ N_{tr}' = N_{tr} g_0\tau_s,$$

$\varepsilon' = \dfrac{\varepsilon}{g\tau_n}$, $\gamma = \dfrac{\tau_n}{\tau_s}$.

It is very useful to rewrite the rate equations in dimensionless units because the normalization considerably simplifies the expressions. Moreover, the number of parameters in the rate equations is also reduced. The normalized rate equations become, respectively:

$$\frac{dN'(t)}{dt} = I' - N'(t) - (N'(t) - N_{tr}')(1 - \varepsilon' S'(t))S'(t) \tag{2.2.1}$$

$$\frac{dS'(t)}{dt} = \gamma(\Gamma(N'(t) - N_{tr}')(1 - \varepsilon' S'(t))S'(t) - S'(t) + \Gamma\beta N'(t)) \tag{2.2.2}$$

where $N'(t)$ and $S'(t)$ are the normalized electron and photon densities, $I'(t)$ is the normalized injection current, Γ is the optical confinement, N'_{tr} is the normalized electron density for transparency, ε' is the normalized gain saturation coefficient, β is the fraction of spontaneous emission, and γ is the ratio of the spontaneous recombination lifetime τ_n to the photon lifetime τ_s.

Table 2.2 Parameters for the Normalized Rate Equations

parameter	value	Unit
β	1.0×10^{-4}	
Γ	0.25	
ε'	8.621×10^{-3}	
N'_{tr}	2.9	
γ	1000	

2.3 Rate Equations Operating Characteristics

2.3.1 Steady State Characteristics

When the injected current density is at a fixed value of $I > I_{th}$, after some possible transient effects such as the turn-on delay and relaxations oscillations, the laser is expected to reach the steady state at which fluctuations of the electron density and photon density are eliminated. The steady-state solution is obtained by setting all time derivatives to zero in the rate equations.

2.3.2 Transient Response

When the laser is turned on by a current I, it required some time for the electron and photon populations to attaining the steady-state. One important feature is the turn-on delay which indicated that stimulated emission does not occur until the electron population reaches its threshold. Another important feature is the relaxation oscillation. The electron and photon population exhibits oscillations before come into equilibrium.

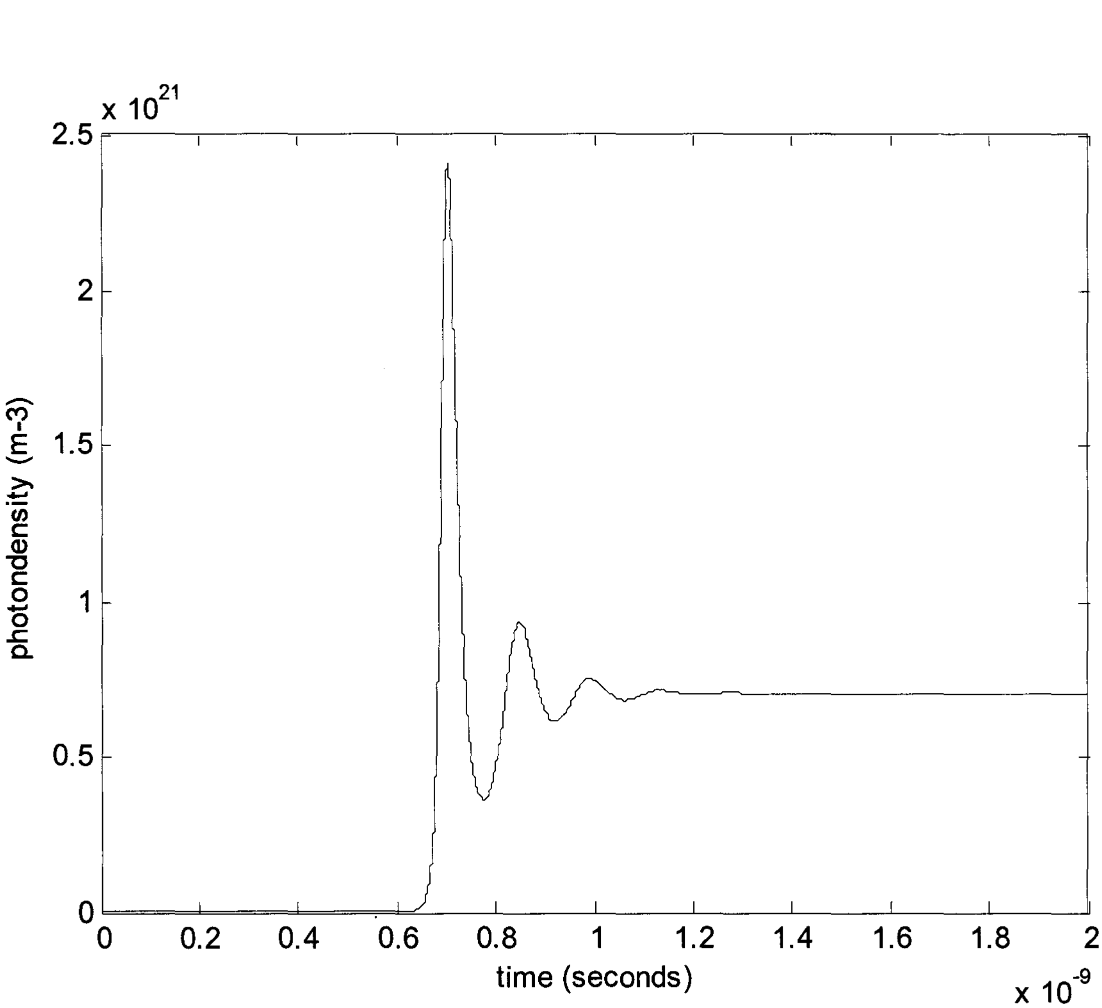

Figure 2.1: Photon densities for DC current injection 37.7mA

2.4 Numerical Large Signal Model

In this section, a numerical model of the single mode rate equations has been introduced to compare to the analytical function solution of rate equations described by the Volterra Series. The Euler method is used in this numerical model to approximate the numerical solutions of the nonlinear differential equations. We know that by definition of finite difference, the approximation of the first-order derivative can be in the forward-difference formula below for some sufficient small value d:

$$f'(a) \approx \lim_{d \to 0} \frac{f(a+d) - f(a)}{d} \tag{2.4.1}$$

Replacing the derivative by the finite difference approximation in the normalized rate equations, we obtained:

$$\frac{N(t+dt) - N(t)}{dt} = I - N(t) - (N(t) - N_{tr})(1 - \varepsilon S(t))S(t) \tag{2.4.2}$$

$$\frac{S(t+dt) - S(t)}{dt} = \gamma(\Gamma(N(t) - N_{tr})(1 - \varepsilon S(t))S(t)) - S(t) + \Gamma\beta N(t) \tag{2.4.3}$$

So that:

$$N_{n+1} = N_n + (I - N_n - (N_n - N_{tr})(1 - \varepsilon S_n)S_n)dt \tag{2.4.4}$$

$$S_{n+1} = S_n + (I - N_n - (N_n - N_{tr})(1 - \varepsilon S_n)S_n)dt \tag{2.4.5}$$

And $N_0 = 0, S_0 = 0$

Using this recursive method, we can obtain the numerical solution of the nonlinear rate equations.

2.4.1 Simulation Result

We use the Euler method to simulate the pulse response for the behaviors of the laser diode. Figure 2.2 and Figure 2.3 below show the input rectangular pulse of 12mA with a bias current of 25.7mA and the output photon density respectively.

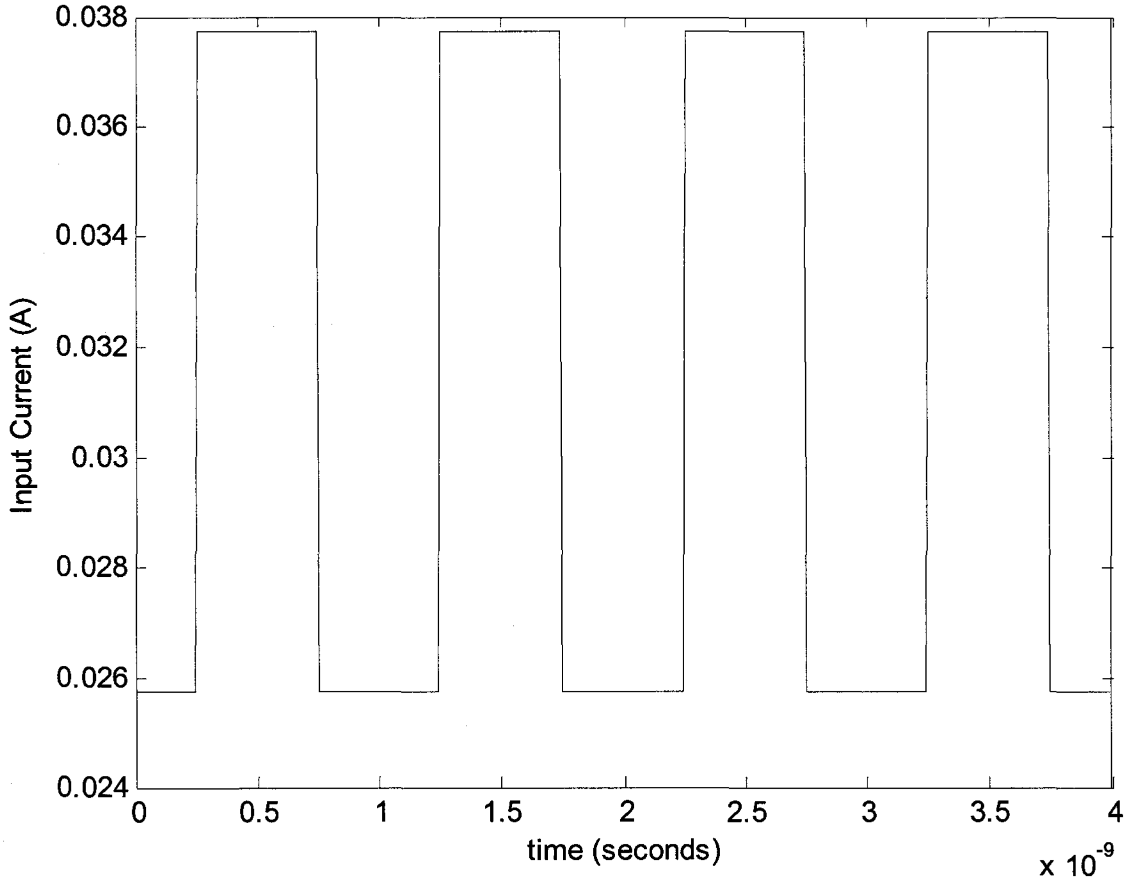

Figure 2.2: Rectangular input pulse with amplitude 12mA on the bias current 25.7mA

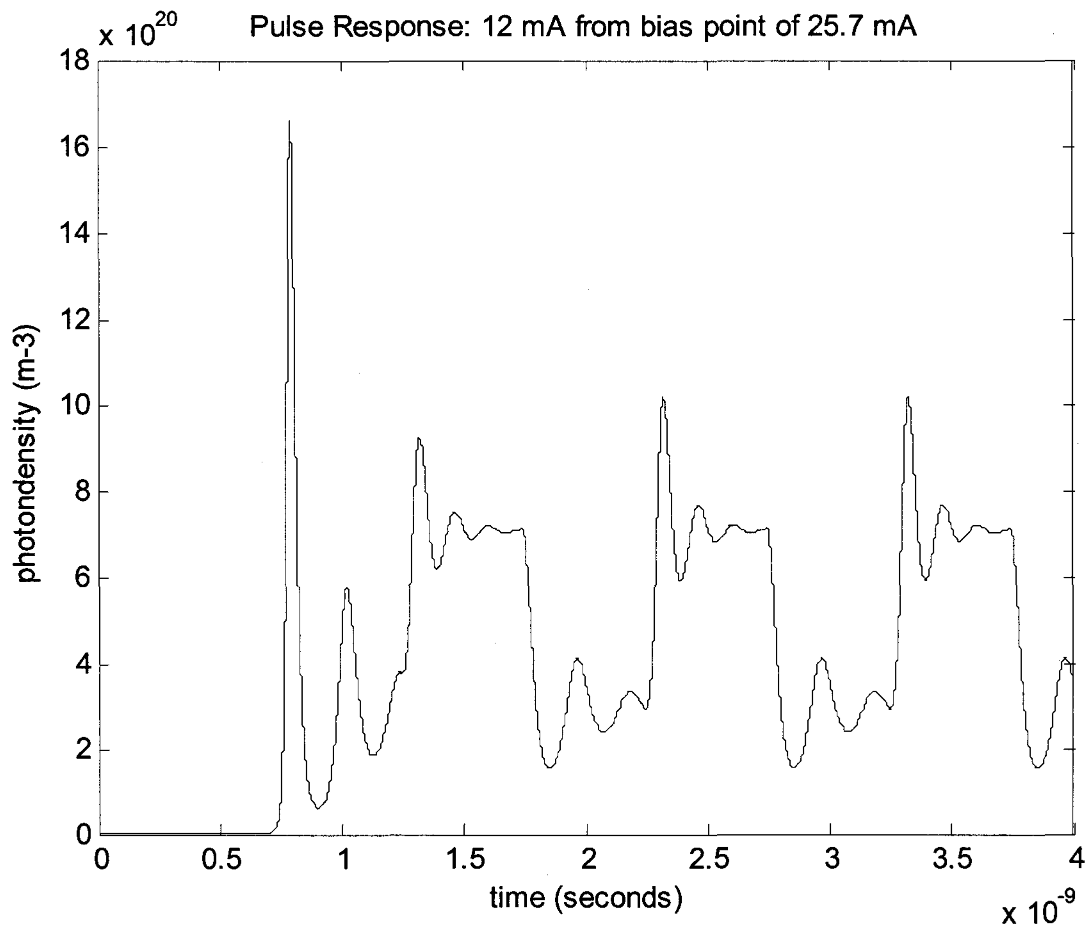

Figure 2.3: Output photon density

2.5 Conclusion

In this chapter, we reviewed the rate equations which govern the relationships between photons and carriers and discuss the dynamic characteristics of the laser diode. We use the numerical method to simulate the behaviors of laser diode. In the thesis, we will neglect the transient response of the laser diode, such as the turn-on delay and relaxation oscillation, which the Volterra Series can not describe. We focus on the characteristic of the laser's nonlinear distortion.

Chapter 3
Small Signal Analysis

3.1 Introduction

The modulation characteristics of the laser diode can be developed by solving the single-mode equations. Under the direct-current modulation, the input current can be written in two parts, one is the bias current I_b and the other is the modulation current ΔI:

$$I(t) = I_b + \Delta I(t) \tag{3.1.1}$$

When the laser is biased above the threshold $I_b > I_{th}$ and the modulation current $\Delta I \ll I_b - I_{th}$, a small signal analysis can be applied in the rate equation. The rate equation can be linearized and solved analytically. And the solution of the small signal model can describe the behavior of the laser diode in a certain extent.

3.2 Linearization of Nonlinear Systems

The procedure of linearization of systems described by nonlinear differential equation is based on the Taylor series expansion [9].

Consider a first-order nonlinear dynamic system in matrix form:

$$\frac{d}{dt}x(t) = F(x(t), u(t)), \tag{3.2.1}$$

Where $x(t)$ is n-dimensional system state space vector, $u(t)$ is the r-dimensional input vector, and F is the n-dimensional vector function.

We assume:

$$x(t) = x_0(t) + \Delta x(t)\,,\quad u(t) = u_0(t) + \Delta u(t)\,,\quad \frac{d}{dt}x_0(t) = F(x_0(t), u_0(t)) \qquad (3.2.2)$$

The right-hand side of the differential equation (3.2.1) can be expanded as follows:

$$\frac{d}{dt}x_0 + \frac{d}{dt}\Delta x = F(x_0 + \Delta x, u_0 + \Delta u) = F(x_0, u_0) + \left(\frac{\partial F}{\partial x}\right)\bigg|_{(x_0,u_0)} \Delta x + \left(\frac{\partial F}{\partial u}\right)\bigg|_{(x_0,u_0)} \Delta u + higher-order$$

$$(3.2.3)$$

The higher-order term can be neglected due to the smaller lever compare to Δx and Δu.

Therefore the approximation of the nonlinear system can be written as the following forms:

$$\frac{d}{dt}\Delta x(t) = \left(\frac{\partial F}{\partial x}\right)\bigg|_{(x_0,u_0)} \Delta x(t) + \left(\frac{\partial F}{\partial u}\right)\bigg|_{(x_0,u_0)} \Delta u(t) \qquad (3.2.4)$$

The partial derivatives are the Jacobian matrices where:

$$\left(\frac{\partial F}{\partial x}\right)\bigg|_{(x_0,u_0)} = \left.\begin{pmatrix} \frac{\partial F_1}{\partial x_1} & \frac{\partial F_1}{\partial x_2} & \cdots & \cdots & \frac{\partial F_1}{\partial x_n} \\ \frac{\partial F_2}{\partial x_2} & \cdots & \cdots & \cdots & \frac{\partial F_2}{\partial x_n} \\ \cdots & \cdots & \frac{\partial F_j}{\partial x_j} & \cdots & \cdots \\ \cdots & \cdots & \cdots & \cdots & \cdots \\ \frac{\partial F_n}{\partial x_1} & \cdots & \cdots & \cdots & \frac{\partial F_n}{\partial x_n} \end{pmatrix}\right|_{(x_0,u_0)} = A \qquad (3.2.5)$$

and

$$(\frac{\partial F}{\partial u})\bigg|_{(x_0,f_0)} = \left.\begin{pmatrix} \frac{\partial F_1}{\partial u_1} & \frac{\partial F_1}{\partial u_2} & \cdots & \cdots & \frac{\partial F_1}{\partial u_n} \\ \frac{\partial F_2}{\partial u_2} & \cdots & \cdots & \cdots & \frac{\partial F_2}{\partial u_n} \\ \cdots & \cdots & \frac{\partial F_j}{\partial u_j} & \cdots & \cdots \\ \cdots & \cdots & \cdots & \cdots & \cdots \\ \frac{\partial F_n}{\partial u_1} & \cdots & \cdots & \cdots & \frac{\partial F_n}{\partial u_n} \end{pmatrix}\right|_{(x_0,u_0)} = B \tag{3.2.6}$$

With these notations, the linearized system can be written as:

$$\frac{d}{dt}\Delta x(t) = A\Delta x(t) + B\Delta u(t) \tag{3.2.7}$$

The output of the nonlinear system satisfies the following equations:

$$y(t) = G(x(t), u(t)) \tag{3.2.8}$$

which can also be expanded into Taylor series:

$$y(t) = y_0(t) + \Delta y(t) = G(x_0, u_0) + (\frac{\partial G}{\partial x})\bigg|_{(x_0,u_0)} \Delta x(t) + (\frac{\partial G}{\partial u})\bigg|_{(x_0,u_0)} \Delta u(t) + higher - order \tag{3.2.9}$$

Neglecting the higher-order term, we assume:

$$C = (\frac{\partial G}{\partial x})\bigg|_{(x_0,u_0)} = \left.\begin{pmatrix} \frac{\partial G_1}{\partial x_1} & \frac{\partial G_1}{\partial x_2} & \cdots & \cdots & \frac{\partial G_1}{\partial x_n} \\ \frac{\partial G_2}{\partial x_2} & \cdots & \cdots & \cdots & \frac{\partial G_2}{\partial x_n} \\ \cdots & \cdots & \frac{\partial G_j}{\partial x_j} & \cdots & \cdots \\ \cdots & \cdots & \cdots & \cdots & \cdots \\ \frac{\partial G_n}{\partial x_1} & \cdots & \cdots & \cdots & \frac{\partial G_n}{\partial x_n} \end{pmatrix}\right|_{(x_0,u_0)} \tag{3.2.10}$$

and

$$D=(\frac{\partial G}{\partial f})\bigg|_{(x_0,u_0)}=\left.\begin{pmatrix} \frac{\partial G_1}{\partial u_1} & \frac{\partial G_1}{\partial u_2} & \cdots & \cdots & \frac{\partial G_1}{\partial u_n} \\ \frac{\partial G_2}{\partial u_2} & \cdots & \cdots & \cdots & \frac{\partial G_2}{\partial u_n} \\ \cdots & \cdots & \frac{\partial G_j}{\partial u_j} & \cdots & \cdots \\ \cdots & \cdots & \cdots & \cdots & \cdots \\ \frac{\partial G_n}{\partial u_1} & \cdots & \cdots & \cdots & \frac{\partial G_n}{\partial u_n} \end{pmatrix}\right|_{(x_0,u_0)} \tag{3.2.11}$$

So that the linearized output equation is obtained:

$$\Delta y(t)=C\Delta x(t)+D\Delta u(t) \tag{3.2.12}$$

And the total output equation is:

$$y(t)=y_0(t)+\Delta y(t) \tag{3.2.13}$$

Finally we obtained the linear state space model:

$$\begin{cases} \frac{d}{dt}\Delta x(t)=A\Delta x(t)+B\Delta u(t) \\ y(t)=y_0+C\Delta x(t)+D\Delta u(t) \end{cases} \tag{3.2.14}$$

3.3 Analysis of the Small Signal Model

When the modulation current is $\Delta I \ll I_b$, an analytical solution can be obtained by linearizing the rate equations. We first choose an arbitrary operating point near threshold and characterize the small signal response of the laser diode by the linearized method showing in the previous section.

Assume $I(t)=I_0+\Delta I(t)$, $N(t)=N_0+\Delta N(t)$ and $S(t)=S_b+\Delta S(t)$, where

(N_0, S_0) is the steady state electron and photon densities for the bias current I_0 Therefore we have $\frac{dN_0}{dt}=0$ and $\frac{dS_0}{dt}=0$. Partial derivatives are taken to the normalized rate equations (2.2.1) and (2.2.2) with respect to $\Delta N(t)$ and $\Delta S(t)$, we obtained:

$$A = \left.\begin{pmatrix} \frac{\partial(\frac{dN(t)}{dt})}{\partial N(t)} & \frac{\partial(\frac{dN(t)}{dt})}{\partial S(t)} \\ \frac{\partial(\frac{dS(t)}{dt})}{\partial N(t)} & \frac{\partial(\frac{dS(t)}{dt})}{\partial S(t)} \end{pmatrix}\right| = \begin{pmatrix} -1-(1-\varepsilon S_0)S_0 & -(N_0-N_{tr})(1-2\varepsilon S_0) \\ \gamma\Gamma(1-\varepsilon S_0)S_0+\gamma\Gamma\beta & \gamma\Gamma(N_0-N_{tr})(1-2\varepsilon S_0)-\gamma \end{pmatrix}$$

(3.3.1)

and

$$B = \left.\begin{pmatrix} \frac{\partial(\frac{dN(t)}{dt})}{\partial I(t)} \\ \frac{\partial(\frac{dS(t)}{dt})}{\partial I(t)} \end{pmatrix}\right|_{(N_0,S_0)} = \begin{pmatrix} 1 \\ 0 \end{pmatrix} \qquad (3.3.2)$$

Now the small signal model is:

$$\begin{pmatrix} \frac{d\Delta N(t)}{dt} \\ \frac{d\Delta S(t)}{dt} \end{pmatrix} = \begin{pmatrix} -1-(1-\varepsilon S_0)S_0 & -(N_0-N_{tr})(1-2\varepsilon S_0) \\ \gamma\Gamma(1-\varepsilon S_0)S_0+\gamma\Gamma\beta & \gamma\Gamma(N_0-N_{tr})(1-2\varepsilon S_0)-\gamma \end{pmatrix} \bullet \begin{pmatrix} \Delta N(t) \\ \Delta S(t) \end{pmatrix} + \begin{pmatrix} 1 \\ 0 \end{pmatrix} \bullet \Delta I(t)$$

(3.3.3)

and the output photon density is:

$$S(t) = \begin{pmatrix} 0 & 1 \end{pmatrix} \begin{pmatrix} \Delta N(t) \\ \Delta S(t) \end{pmatrix} + S_0$$

(3.3.4)

3.4 Frequency Domain Representation

The frequency responses of the small signal model can be determined from the linearized rate equations (2.2.1) and(2.2.2). The transfer function for intensity modulation is the output signal to the input signal in the frequency domain.

$$\frac{d\Delta N(t)}{dt}=(-1-(1-\varepsilon S_0)S_0)\Delta N(t)-(N_0-N_{tr})(1-2\varepsilon S_0)\Delta S(t)+\Delta I(t) \qquad (3.4.1)$$

$$\frac{d\Delta S(t)}{dt}=(\gamma\Gamma(1-\varepsilon S_0)S_0+\gamma\Gamma\beta)\Delta N(t)+(\gamma\Gamma(N_0-N_{tr})(1-2\varepsilon S_0)-\gamma)\Delta S(t) \qquad (3.4.2)$$

Taking Fourier Transform on the both side of the equations (3.4.1) and(3.4.2):

$$j\omega\Delta N(j\omega)=(-1-(1-\varepsilon S_0)S_0)\Delta N(j\omega)-(N_0-N_{tr})(1-2\varepsilon S_0)\Delta S(j\omega) \qquad (3.4.3)$$

$$j\omega S(j\omega)=(\gamma\Gamma(1-\varepsilon S_0)S_0+\gamma\Gamma\beta)\Delta N(j\omega)+(\gamma\Gamma(N_0-N_{tr})(1-2\varepsilon S_0)-\gamma)\Delta S(j\omega) \quad (3.4.4)$$

Then we obtain the transfer function for the photon density is

$$H(j\omega)=\frac{\Delta S(j\omega)}{\Delta I(j\omega)}$$

$$=\frac{\gamma\Gamma((1-\varepsilon S_0)S_0+\beta)}{(j\omega+1+(1-\varepsilon S_0)S_0)(j\omega+\gamma(\Gamma(N_0-N_{tr})(1-2\varepsilon S_0)-1))+\gamma\Gamma(N_0-N_{tr})(1-2\varepsilon P_0)(\beta+(1-\varepsilon P_0)P_0)}$$

(3.4.5)

And the transfer function for the carrier density is:

$$G(j\omega)=\frac{\Delta N(j\omega)}{\Delta I(j\omega)}$$

$$=\frac{j\omega-\gamma(\Gamma(N_0-N_{tr})(1-2\varepsilon S_0)-1)}{(j\omega+1+(1-\varepsilon S_0)S_0)(j\omega+\gamma(\Gamma(N_0-N_{tr})(1-2\varepsilon S_0)-1))+\gamma\Gamma(N_0-N_{tr})(1-2\varepsilon P_0)(\beta+(1-\varepsilon P_0)P_0)}$$

(3.4.6)

3.4.1 Simulation Result

We simulate the linear model case and set up a bias current near the threshold point $I_b = 1.3 I_{th}$. The transfer function of the photon density in the linear model is as below:

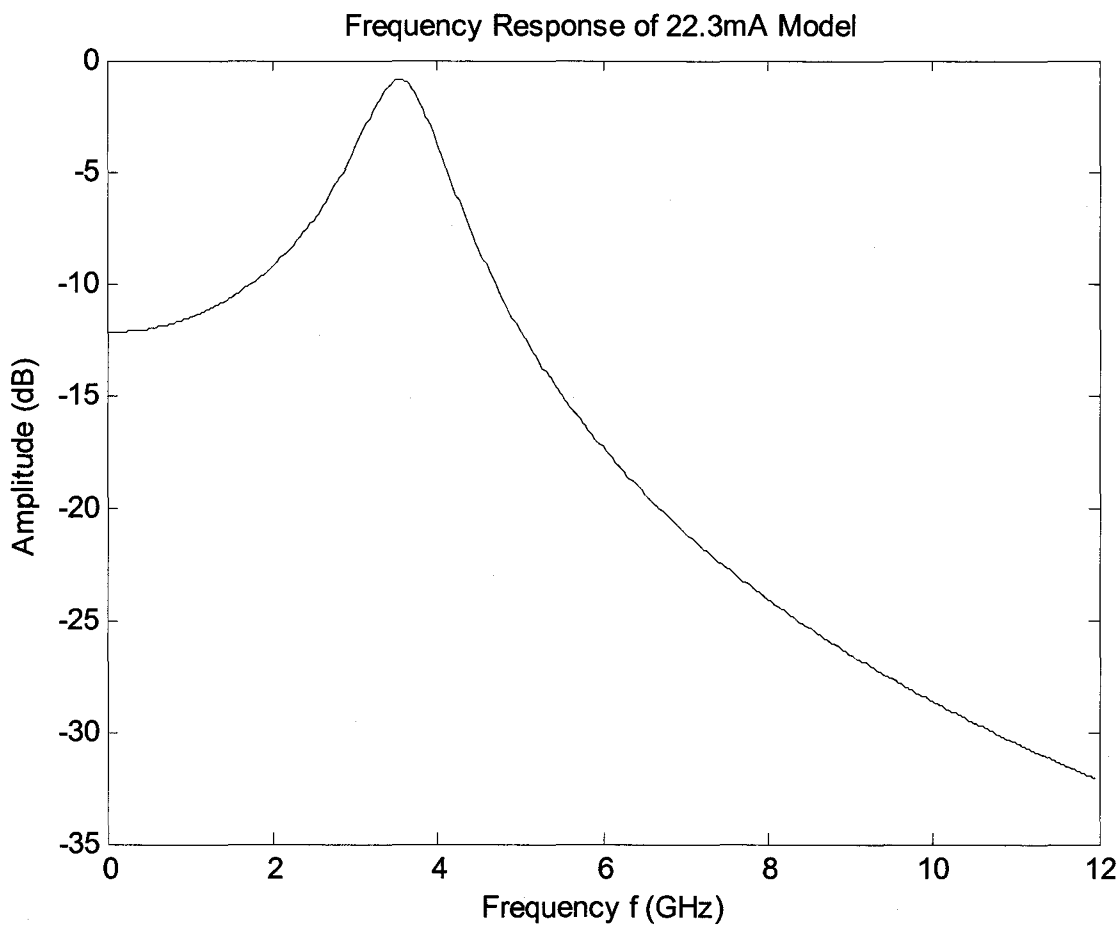

Figure 3.1: Magnitude response of the bias current 22.3mA

Let the input signal be the rectangular pulse of amplitude A on the bias current $I_0 = 1.3I_{th} = 22.3mA$. When the modulated current amplitude ΔI is small enough compared to the bias current, the linear model has a good description of the distortion characteristics of the laser diode.

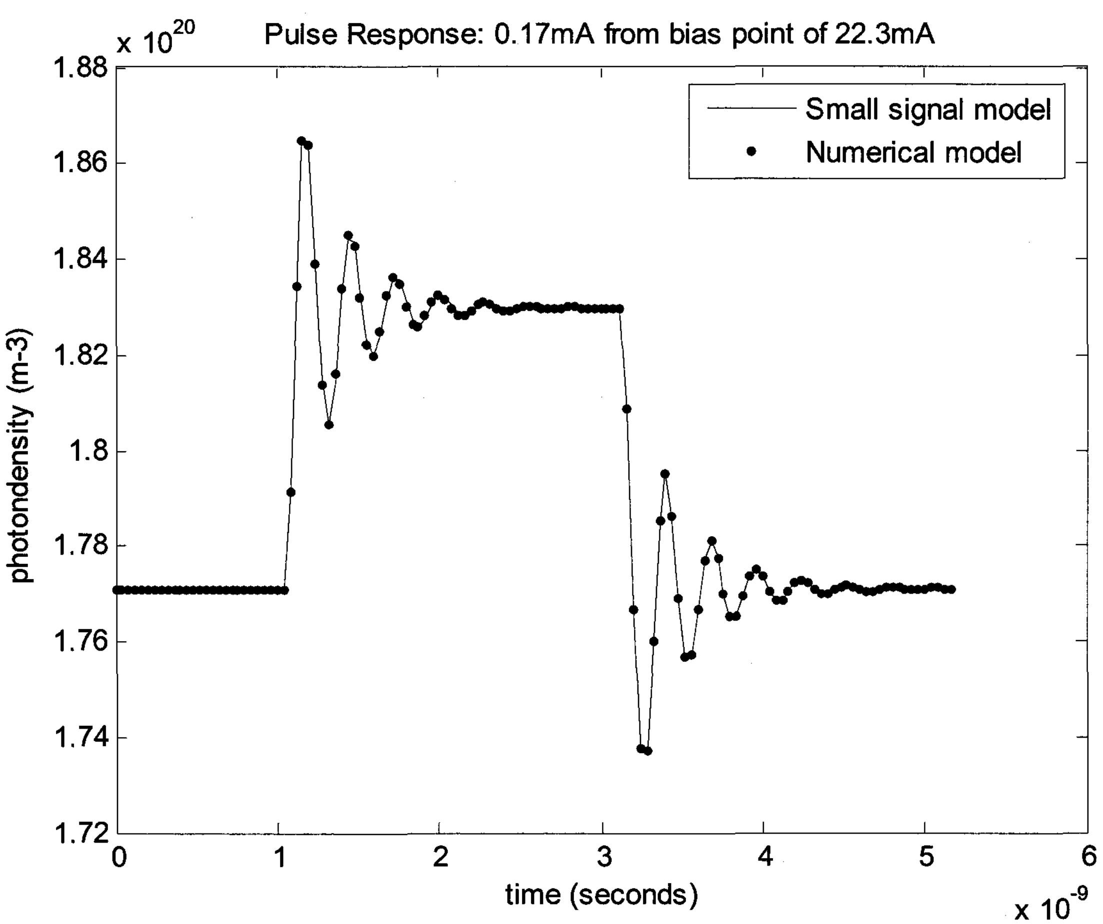

Figure 3.2: Small signal response to rectangular pulse with amplitude 0.17mA biased on the current 22.3mA

In Figure 3.2, we find out that the two curves fit well when the modulated current $\Delta I = 0.17mA$ is far less than the bias current $I_0 = 22.3mA$. Therefore for any modulated current $\Delta I \ll I_0$, the small signal analysis is a useful method which depicts the modulation response characteristics well.

The next step we increase the amplitude of the modulated rectangular pulse based on the same operating points.

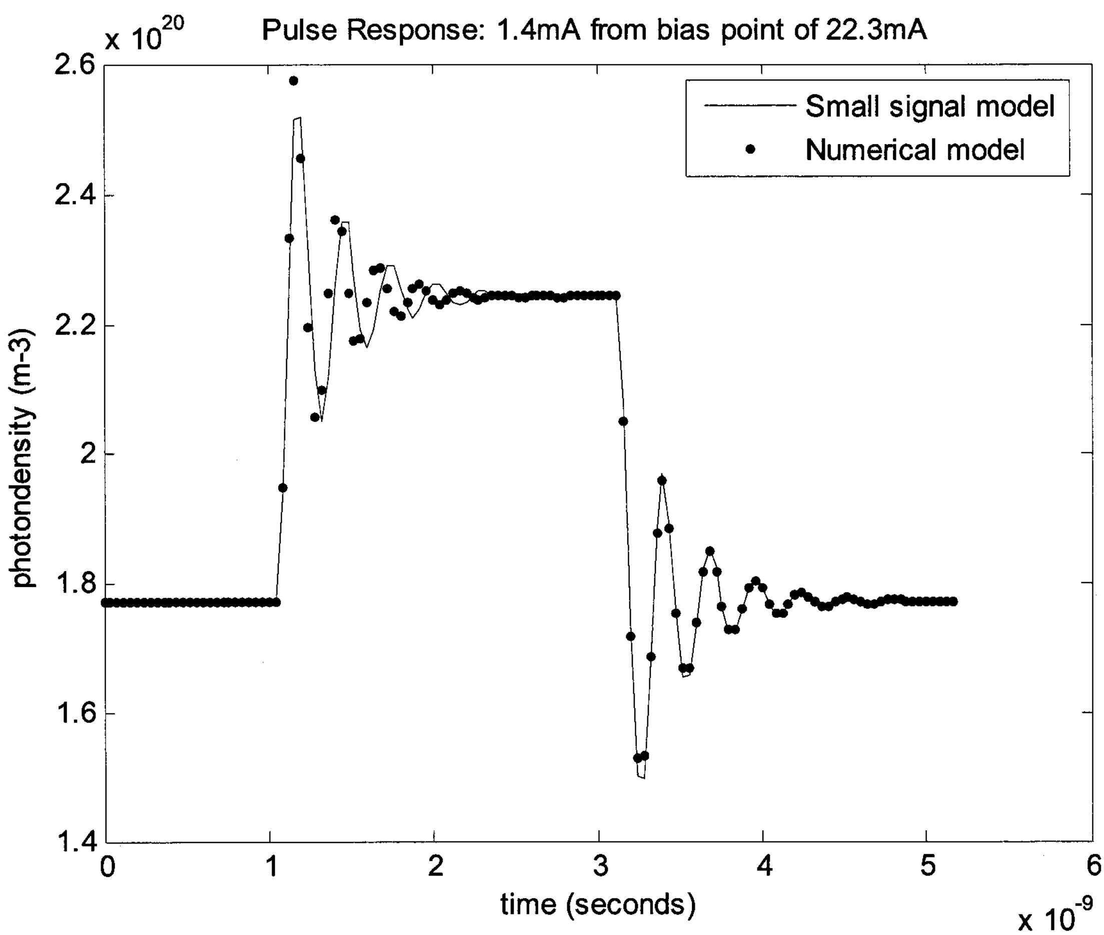

Figure3.3: Small signal response to rectangular pulse with amplitude 1.4mA biased on the current 22.3mA

As shown in Figure 3.3, when the modulated current amplitude increased from $0.17mA$ to $1.4mA$, the small signal model has some errors to describe the modulation response of the laser response.

3.5 Linear Signal Distortion Compensation

Given a transfer function of a linear time invariant system $F(s)$, we can find that the inverse system transfer function $F^{inv}(s)$ satisfies:

$$F^{inv}(s) \bullet F(s) = 1 \tag{3.5.1}$$

If $F(s)$ is written in pole-zero form:

$$F(s) = \frac{\prod_k (A_k s - d_k)}{\prod_k (B_k s - c_k)} \tag{3.5.2}$$

Let us discuss the stable and causal of the inverse system with the transfer function $F^{inv}(s)$. We have got the conclusion that a stable, causal system must have all its poles in the left half of the s-plan. Therefore, if all the zeros of $F(s)$ are in the left half of the s-plan, the inverse system with the transfer function $F^{inv}(s)$ is stable and causal.

According to the conclusion above, we find out that the inverse of the linearized model of the rate equations exists. To compensate the linear distortion, the inverse transfer function must satisfy the equation that $H^{inv}(f) \bullet H(f) = H_1(0)$. Therefore, the linear inverse transfer function is derived:

$$K(f) = H_1(0) H_1^{-1}(f)$$

3.5.1 Simulation Result

The Figure 3.4 below shows an input rectangular pulse with amplitude $\Delta I = 0.01Ith$ on a bias current $I_0 = 1.3Ith$. Figure 3.5 shows the pulse response of the second-order linear system with a transfer function $H(f)$. Then we calculate the gain and design the inverse transfer function $H(f)$ to cancel the oscillation in the output pulse in Figure 3.6:

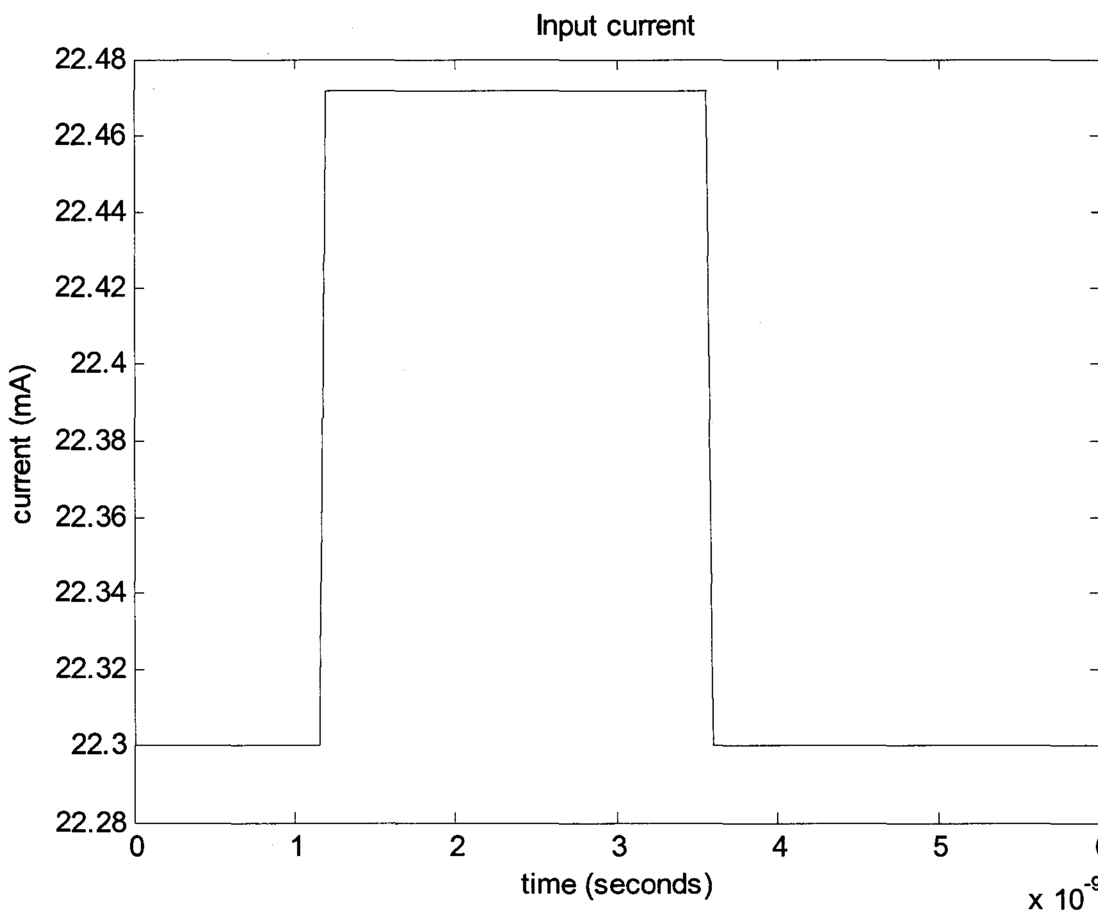

Figure 3.4: Input rectangular pulse with amplitude 0.17mA biased on 22.3mA

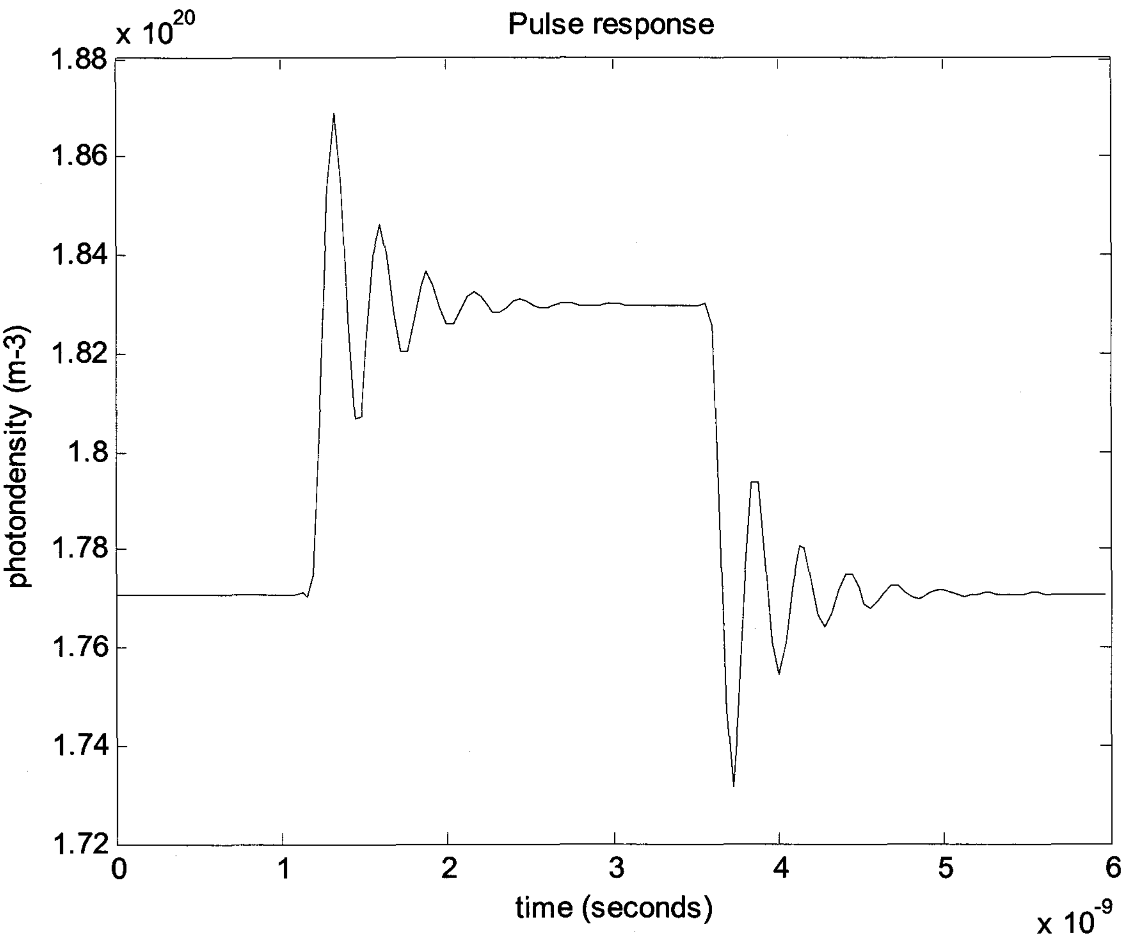

Figure 3.5: Output pulse of the small signal model

Let the signal in Figure 3.5 be the input of the inverse system K, the reshaped signal is shown in Figure 3.6.

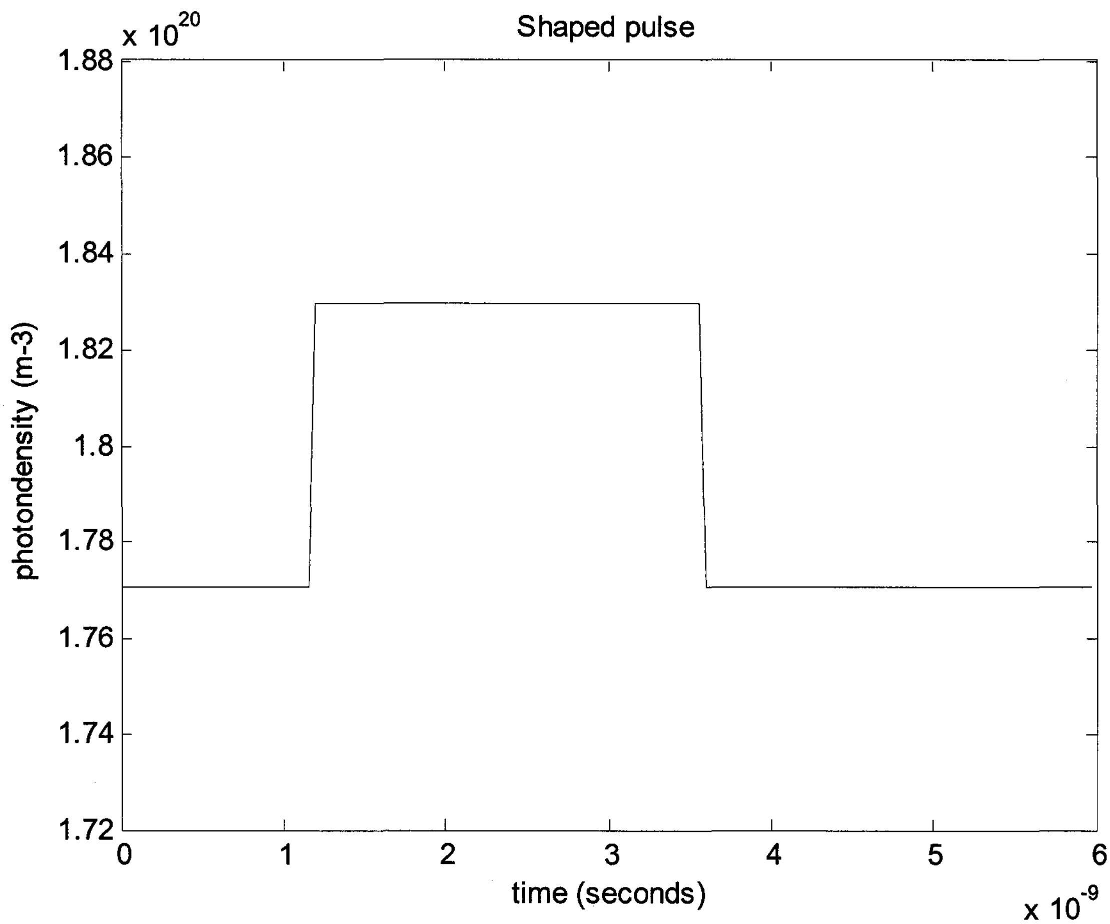

Figure 3.6: Reshaped output signal of the small signal model

3.6 Conclusion

The semiconductor lasers can be directly modulated by modulating the injection current. The small-signal analysis is conducted to understand the laser modulation characteristics in the relative linear region above threshold by linearizing the rate equations. However, the small analysis is not necessarily valid when the modulated injection current increases sufficiently large. And then the nonlinear effects play an important role which can be described well in a large signal model.

Chapter 4
Volterra Series Analysis

4.1 Background

The small signal model has some limitations to describe the modulation response of the laser diode when the modulated current is large enough, which leads to the discrepancy between the analytical model solutions and the numerical solutions of the rate equation. So the Volterra series is introduced into the large signal model to analyze the nonlinearities distortion of the laser diode. The Volterra series can portray the laser's non-linearity distortion more accurately compared to the small signal model and in a more tolerant condition.

4.2 Volterra Series Representations

The Volterra series provide an analytical approach based on the functional expansion to model a time-invariant nonlinear system with memory. We can present the output of the nonlinear system with a power series of the input using the Volterra Series. It can be expressed as:

$$y(t) = h_0 + \int_{-\infty}^{+\infty} h_1(\tau_1)x(t-\tau_1)d\tau_1$$

$$+\int_{-\infty}^{+\infty}\int_{-\infty}^{+\infty} h_2(\tau_1,\tau_2)x(t-\tau_1)x(t-\tau_2)d\tau_1 d\tau_2$$

$$+\ldots$$
$$+\int_{-\infty}^{+\infty}\ldots\int_{-\infty}^{+\infty}h_n(\tau_1,\tau_2,\ldots\tau_n)x(t-\tau_1)x(t-\tau_2)\ldots x(t-\tau_n)d\tau_1 d\tau_2\ldots d\tau_n+\ldots. \quad (4.2.1)$$

where $x(t)$ is the input, $y(t)$ is the output, and $h_i(\tau_1,\tau_2\ldots\tau_i)$ is the ith-order Volterra kernel of the system. It is obvious that, for n=1, $h_1(\tau_1)$ is the impulse response for the linear, causal system with memory.

Taking multidimensional Fourier Transform on the nth Volterra kernels, we obtain the nth order transfer function as the following forms in the frequency domain analysis:

$$H_n(f_1,f_2\ldots f_n)=\int_{-\infty}^{+\infty}\ldots\int_{-\infty}^{+\infty}h_n(\tau_1,\tau_2,\ldots\tau_n)\exp(-j2\pi(f_1\tau_1+f_2\tau_2+\ldots+f_n\tau_n))d\tau_1 d\tau_2\ldots d\tau_n \quad (4.2.2)$$

and

$$h_n(t_1,t_2\ldots t_n)=\int_{-\infty}^{+\infty}\ldots\int_{-\infty}^{+\infty}H_n(\tau_1,\tau_2,\ldots\tau_n)\exp(j2\pi(f_1\tau_1+f_2\tau_2+\ldots+f_n\tau_n))df_1 df_2\ldots df_n \quad (4.2.3)$$

Therefore $y(t)$ has the other representation as follows:

$$y(t)=h_0+\int_{-\infty}^{+\infty}H_1(f_1)X(f_1)\exp(j2\pi f_1 t)df_1$$
$$+\int_{-\infty}^{+\infty}\int_{-\infty}^{+\infty}H_2(f_1,f_2)X(f_1)X(f_2)\exp(j2\pi(f_1+f_2)t)df_1 df_2$$
$$+\ldots$$
$$+\int_{-\infty}^{+\infty}\ldots\int_{-\infty}^{+\infty}H_n(f_1,f_2\ldots f_3)\prod_{i=1}^{n}X(f_i)\exp(j2\pi f_i t)df_i \quad (4.2.4)$$

In general, the first few terms of the Volterra Series expansion can characterize the output $y(t)$ well if the nonlinearities of the system are not too violent.

4.3 Determination of the Volterra Kernels

When the equations describing the relationship between the input $x(t)$ and $y(t)$ are known, there are several techniques to measure the Volterra kernels $h_n(\tau_1,\tau_2...\tau_n)$ or $H_n(f_1,f_2...f_n)$. In this section, a convenient method called 'probing' or 'the harmonic input' method is introduced to evaluate the nonlinear transfer function [8].

Moreover, here we can assume the kernels of the nonlinear system be symmetric without loss of generality. The transfer functions are the same due to the permutation of the orders of frequency components, which means $H_n(f_{k1},f_{k2}...f_{kn})=H_n(f_{m1},f_{m2}...f_{mn})$, the vectors $(f_{k1},f_{k2}...f_{kn})$ and $(f_{m1},f_{m2}...f_{mn})$ are only different in the orders of the each component.

Let the input $x(t)$ to the nonlinear system be a sum of exponentials:

$$x(t)=\exp(j2\pi f_1 t)+\exp(j2\pi f_2 t)+...\exp(j2\pi f_n t) \tag{4.3.1}$$

With its Fourier transform as follows:

$$X(\xi)=\delta(\xi-f_1)+\delta(\xi-f_2)+...\delta(\xi-f_n) \tag{4.3.2}$$

Substituting $X(\xi)$ into equation(4.2.4), we obtain the output of the nonlinear system:

$$y(t)=\sum_{n=1}^{\infty}\int...\int_{-\infty}^{+\infty}H_n(\xi_1,\xi_2...\xi_n)\prod_{i=1}^{n}[\delta(\xi_i-f_1)+\delta(\xi_i-f_2)+...\delta(\xi_i-f_n)]\exp(j2\pi\xi_i t)d\xi_i$$

(4.3.3)

Expand $\prod_{i=1}^{n}[\delta(\xi_i-f_1)+\delta(\xi_i-f_2)+...\delta(\xi_i-f_n)]$ into polynomial, we obtain

$$\prod_{i=1}^{n}[\delta(\xi_i - f_1)+\delta(\xi_i - f_2)+...\delta(\xi_i - f_n)] = \sum_m \frac{n!}{m_1!m_2!...m_n!}(\delta(\xi_1 - f_{k1})\delta(\xi_2 - f_{k2})...\delta(\xi_n - f_{kn}))$$

(4.3.4)

where $\sum_{i=1}^{n} m_i = n$.

Therefore, we obtain the following form of output:

$$y(t) = \sum_{n=1}^{\infty} \int ... \int_{-\infty}^{+\infty} H_n(\xi_1, \xi_2 ... \xi_n) \sum_m \frac{n!}{m_1!m_2!...m_n!}(\delta(\xi_1 - f_{k1})\delta(\xi_2 - f_{k2})...\delta(\xi_n - f_{kn}))$$

$$= \sum_{n=1}^{\infty} \sum_m \frac{n!}{m_1!m_2!...m_n!} H_n(f_{k1}, f_{k2} ... f_{kn}) \exp(j2\pi(f_{k1} + f_{k2} + ... f_{kn})) \qquad (4.3.5)$$

When the frequencies $f_{k1}, f_{k2} ... f_{kn}$ are distinct from each other, that is, $m_1 = m_2 = ... = m_n = 1$, we can derive the analytical nth-order transfer function from the output terms with coefficient of $n! \exp(j2\pi(f_{k1} + f_{k2} + ... f_{kn}))$.

4.4 Perturbation Technique in Rate Equations

In this section, a perturbation technique [1] will be used to separate the injection current to the laser diode into a 'dc' term which is above the threshold current and a time varying term. The final equations will describe the perturbation of the photon and electron density in terms of an arbitrary steady state value.

Let $I = I_0 + I(t)$, $N = N_0 + N(t)$ and $S = S_0 + S(t)$ where N_0, S_0 is the steady state solution of I_0. The overall rate equations follow:

$$\frac{dN}{dt}=\frac{d(N_0+N(t))}{dt}=(I_0+I(t))-(N_0+N(t))-((N_0+N(t))-N_{tr})(1-\varepsilon(S_0+S(t)))(S_0+S(t))$$

(4.4.1)

$$\frac{dS}{dt}=\frac{d(S_0+S(t))}{dt}=\gamma(\Gamma((N_0+N(t))-N_{tr})(1-\varepsilon(S_0+S(t)))(S_0+S(t))-(S_0+S(t))+\Gamma\beta(N_0+N(t)))$$

(4.4.2)

For the dc component, we have:

$$\frac{dN_0}{dt}=I_0-N_0-(N_0-N_{tr})(1-\varepsilon S_0)S_0=0 \tag{4.4.3}$$

$$\frac{dS_0}{dt}=\gamma(\Gamma(N_0-N_{tr})(1-\varepsilon S_0)S_0-S_0+\Gamma\beta N_0)=0 \tag{4.4.4}$$

The differential equations about the time varying term $N(t),S(t)$ are as follows,

$$\begin{aligned}\frac{dN(t)}{dt}&=I(t)-((1-\varepsilon S_0)S_0+1)N(t)-(N_0-N_{tr})(1-2\varepsilon S_0)S(t)\\&\quad-(1-2\varepsilon S_0)N(t)S(t)+(N_0-N_{tr})\varepsilon S^2(t)+\varepsilon N(t)S^2(t)\end{aligned} \tag{4.4.5}$$

$$\begin{aligned}\frac{dS(t)}{dt}&=\gamma(\Gamma(N_0-N_{tr})(1-2\varepsilon S_0)-1)S(t)+\gamma\Gamma((1-\varepsilon S_0)S_0+\beta)N(t)\\&\quad+\gamma\Gamma(1-2\varepsilon S_0)S(t)N(t)-\gamma\Gamma(N_0-N_{tr})\varepsilon S^2(t)-\gamma\Gamma\varepsilon N(t)S^2(t)\end{aligned} \tag{4.4.6}$$

4.5 Derivation of the First-order Kernel of Rate Equations

Using the Probing Method discussed in section 4.3, we first find out the first-order transfer function of the rate equation by an exponential input.

Let $I(t)=\exp(j2\pi ft)$, according to equation(4.3.5), the output $N(t),S(t)$ must satisfy the equations below:

$$N(t)=G_1(f)\exp(j2\pi ft) \tag{4.5.1}$$

$$S(t)=H_1(f)\exp(j2\pi ft) \tag{4.5.2}$$

Substituting $N(t),S(t)$ into the differential equations(4.4.5) and(4.4.6), and finding out all terms with the coefficients $1!\exp(j2\pi f_1 t)$, then the first-order transfer function is determined:

$$j2\pi f G_1(f) = 1 - ((1-\varepsilon S_0)S_0 + 1)G_1(f) - (N_0 - N_{tr})(1-2\varepsilon S_0)H_1(f) \quad (4.5.3)$$

$$j2\pi f H_1(f) = \gamma(\Gamma(N_0 - N_{tr})(1-2\varepsilon S_0) - 1)H_1(f) + \gamma\Gamma((1-\varepsilon S_0)S_0 + \beta)G_1(f) \quad (4.5.4)$$

Solving the equations, we obtain:

$$H_1(f) = \frac{\gamma\Gamma((1-\varepsilon S_0)S_0+\beta)}{(j2\pi f+(1-\varepsilon S_0)S_0+1)(j2\pi f-\gamma(\Gamma(N_0-N_{tr})(1-2\varepsilon S_0)-1))+\gamma\Gamma(N_0-N_{tr})(1-2\varepsilon S_0)((1-\varepsilon S_0)S_0+\beta)} \quad (4.5.5)$$

$$G_1(f) = \frac{j2\pi f-\gamma(\Gamma(N_0-N_{tr})(1-2\varepsilon S_0)-1)}{(j2\pi f+(1-\varepsilon S_0)S_0+1)(j2\pi f-\gamma(\Gamma(N_0-N_{tr})(1-2\varepsilon S_0)-1))+\gamma\Gamma(N_0-N_{tr})(1-2\varepsilon S_0)((1-\varepsilon S_0)S_0+\beta)} \quad (4.5.6)$$

It is easy to verify that the first-order transfer functions are the same with the transfer functions of the small signal model. That is to say, the first-order transfer functions can be recognized as the transfer function of the linear, causal system with memory.

4.5.1 Simulation Result

In this section, we simulate the laser's response to a modulated rectangular pulse using the first-order transfer function. We compare the analytical result and the numerical result on the same bias currents and the modulated current amplitudes.

First, we let input signal amplitude $\Delta I = 0.6Ith$ with a bias current $I_b = 3Ith$.

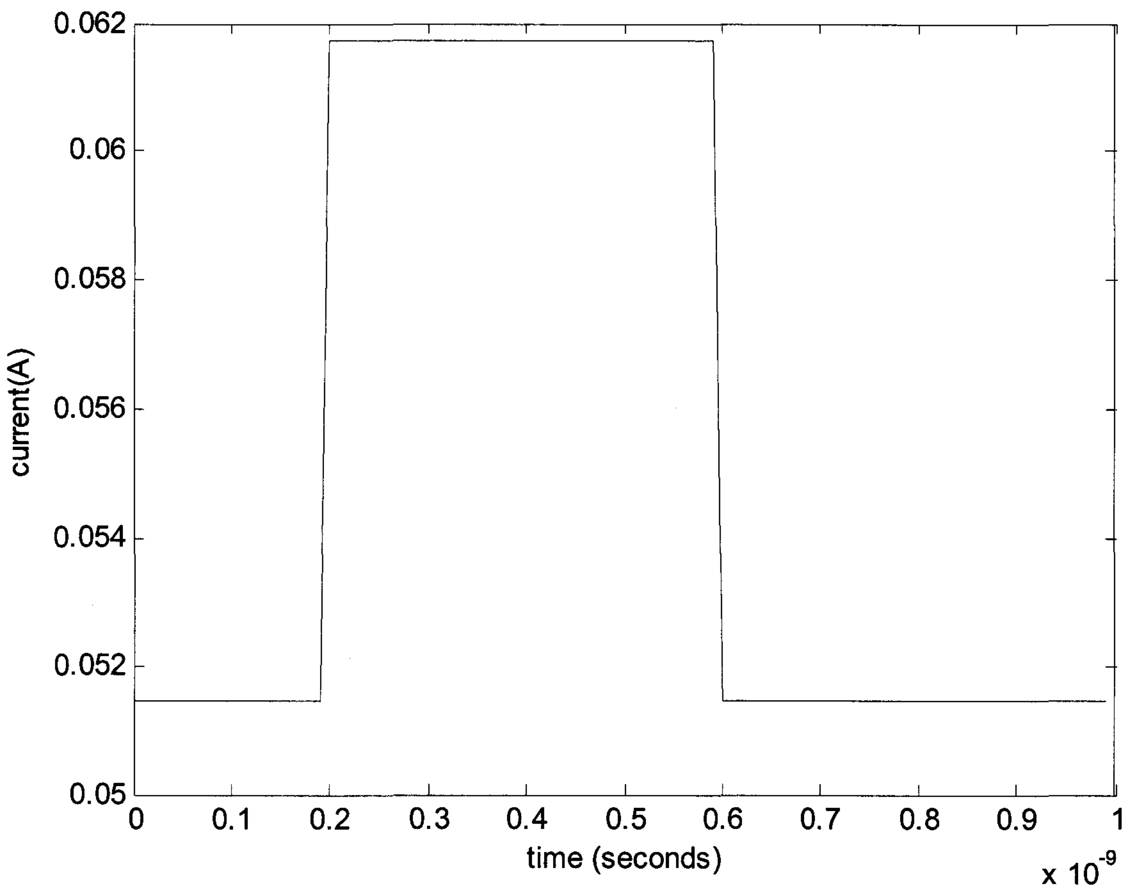

Figure 4.1: Input signal with modulated current amplitude 10.3 mA biased on the current 51.5 mA

The analytical first order output signal compared with the numerical solution is in the figure below:

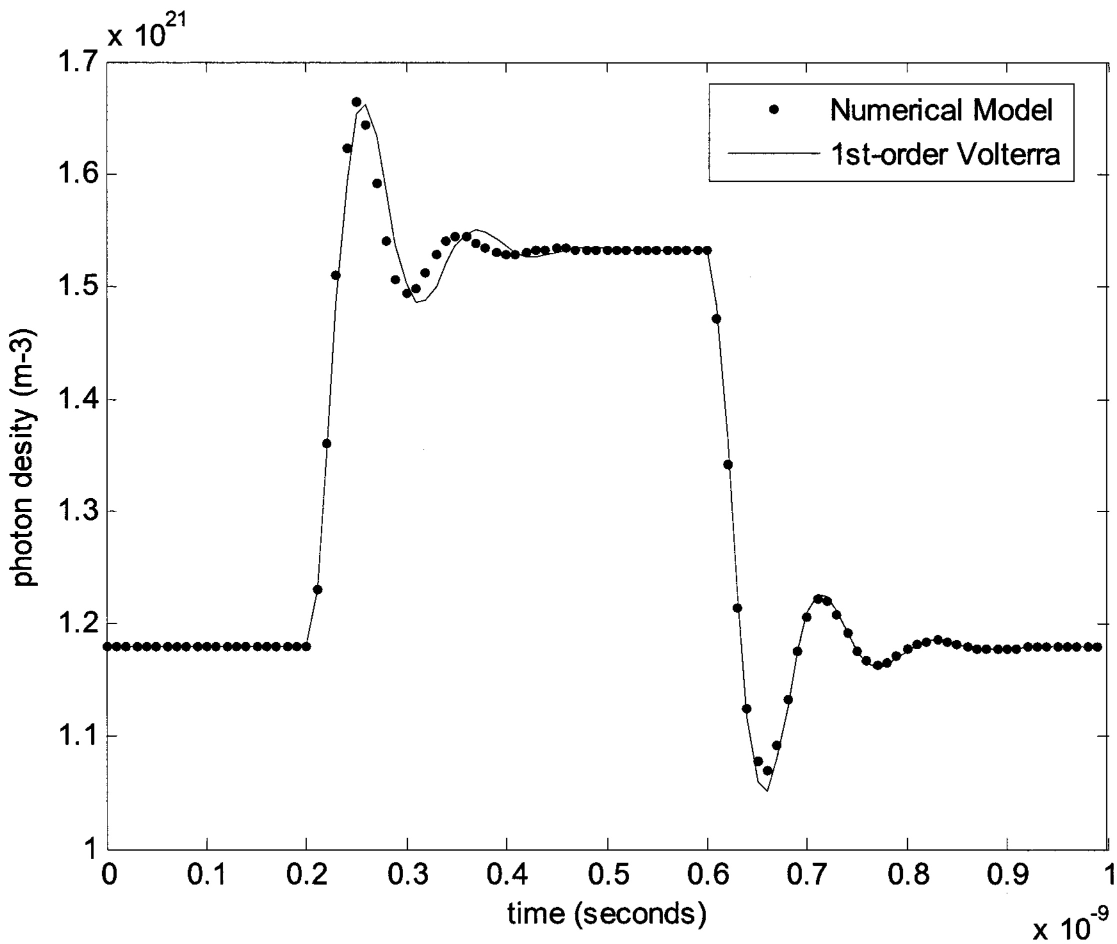

Figure 4.2: Output signal describe by the first-order Volterra model

Here we define a global error function to describe the discrepancy between the Volterra model and the numerical model.

$$GlobalError = \frac{[\int_0^t dt \left| P_N(t) - P_A(t) \right|^2]^{1/2}}{\int_0^t P_N(t)dt} \tag{4.5.7}$$

Where $P_N(t)$ is the numerical photon density and $P_A(t)$ is the analytical photon density described by Volterra series. We test the error between the first-order analytical solution and the numerical solution on the various modulated current amplitude based on the bias current $I_0 = 3I_{th}$

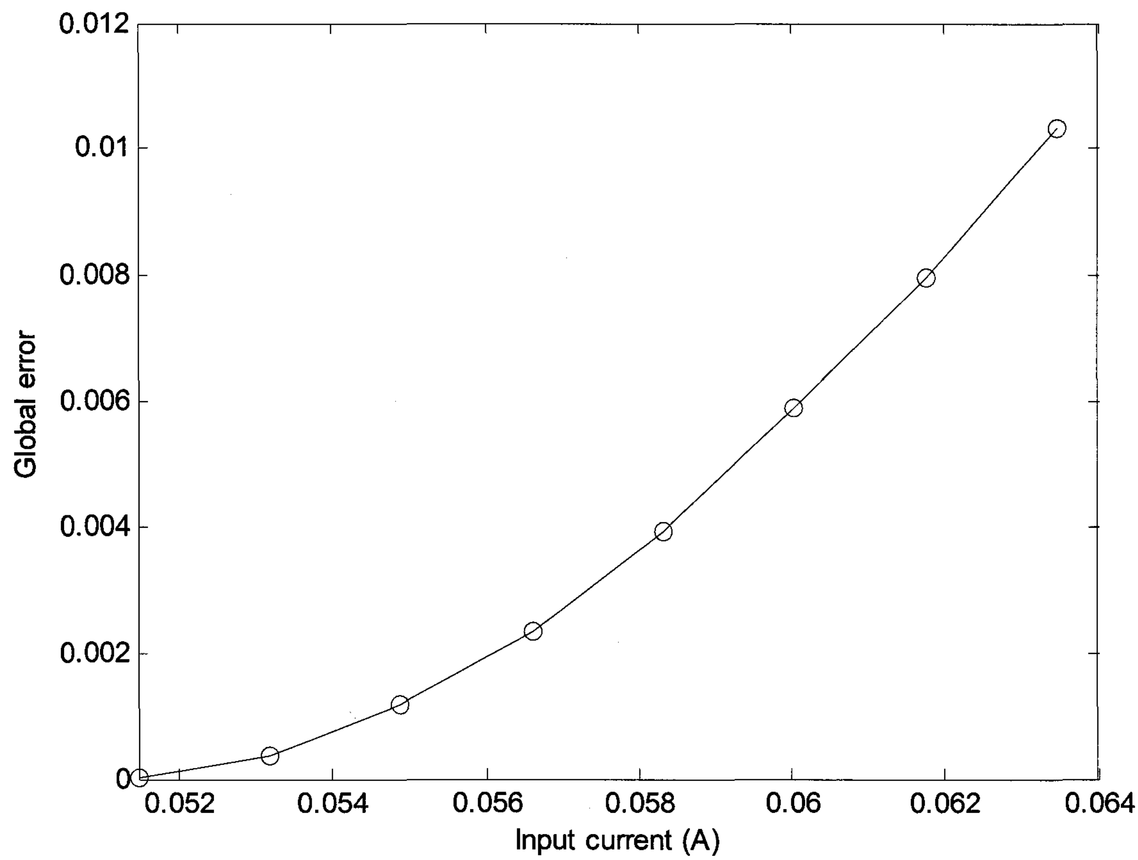

Figure 4.3: Global error between the first-order Volterra and numerical model

The first-order error will be compared to the second-order error in the next section to show the accuracy improvement by the higher order Volterra series.

4.6 Derivation of the Second-order Kernel of Rate Equations

Solving for the second-order transfer function, the procedure is similar with the first-order one but with the sum of two exponentials as input:

Let the input $I(t) = \exp(j2\pi f_1 t) + \exp(j2\pi f_2 t)$, according to equation(4.3.5), the relationship between the output $N(t), S(t)$ and input $I(t)$ satisfies:

$$\begin{aligned} N(t) &= G_1(f_1)\exp(j2\pi f_1 t) + G_1(f_2)\exp(j2\pi f_2 t) \\ &\quad +2G_2(f_1, f_2)\exp(j2\pi(f_1+f_2)t) + G_2(f_1, f_1)\exp(j4\pi f_1 t) + G_2(f_2, f_2)\exp(j4\pi f_2 t) \end{aligned} \tag{4.6.1}$$

$$\begin{aligned} S(t) &= H_1(f_1)\exp(j2\pi f_1 t) + H_1(f_2)\exp(j2\pi f_2 t) \\ &\quad +2H_2(f_1, f_2)\exp(j2\pi(f_1+f_2)t) + H_2(f_1, f_1)\exp(j4\pi f_1 t) + H_2(f_2, f_2)\exp(j4\pi f_2 t) \end{aligned} \tag{4.6.2}$$

Repeat the same process as extracting the first-order transfer function. Substituting $N(t), S(t)$ into the nonlinear rate equation, and finding out all the terms with the coefficients $2!\exp(j2\pi(f_1+f_2)t)$, then the first-order transfer function is determined by:

$$\begin{aligned} &(j2\pi(f_1+f_2) + (1-\varepsilon S_0)S_0 + 1)G_2(f_1, f_2) \\ &= -(N_0 - N_{tr})(1-2\varepsilon S_0)H_2(f_1, f_2) \\ &\quad -\frac{1}{2}(1-2\varepsilon S_0)(G_1(f_1)H_1(f_2) + G_1(f_2)H_1(f_1)) + (N_0 - N_{tr})\varepsilon H_1(f_1)H_1(f_2) \end{aligned} \tag{4.6.3}$$

and

$$(j2\pi(f_1+f_2)-\gamma(\Gamma(N_0-N_{tr})(1-2\varepsilon S_0)-1))H_2(f_1,f_2)$$
$$=\gamma\Gamma((1-\varepsilon S_0)S_0+\beta)G_2(f_1,f_2)$$
$$+\frac{1}{2}\gamma\Gamma(1-2\varepsilon S_0)(G_1(f_1)H_1(f_2)+G_1(f_2)H_1(f_1))-\gamma\Gamma\varepsilon(N_0-N_{tr})H_1(f_1)H_1(f_2) \quad (4.6.4)$$

Solving the equations, the second-order transfer function has been obtained:

Let $a=j2\pi(f_1+f_2)+(1-\varepsilon S_0)S_0+1$ (4.6.5)

$$b=j2\pi(f_1+f_2)-\gamma(\Gamma(N_0-N_{tr})(1-2\varepsilon S_0)-1) \quad (4.6.6)$$

$$c=ab+\gamma\Gamma(N_0-N_{tr})(1-2\varepsilon S_0)((1-\varepsilon S_0)S_0+\beta) \quad (4.6.7)$$

$$d=\frac{1}{2}(1-2\varepsilon S_0)(G_1(f_1)H_1(f_2)+G_1(f_2)H_1(f_1))-(N_0-N_{tr})\varepsilon H_1(f_1)H_1(f_2) \quad (4.6.8)$$

We obtain:

$$H_2(f_1,f_2)=\frac{\gamma\Gamma d}{c}(a-((1-\varepsilon S_0)S_0+\beta)) \quad (4.6.9)$$
$$G_2(f_1,f_2)=-\frac{d}{c}(\gamma\Gamma(N_0-N_{tr})(1-2\varepsilon S_0)+b) \quad (4.6.10)$$

4.6.1 Simulation Result

We used the same bias current amplitude $I_b=3Ith$ and modulation current amplitude $\Delta I=0.6Ith$ as we did in the first-order Volterra analysis. Figure 4.4 shows the second-order nonlinear distortion of the rectangular input pulse in the second-order Volterra model.

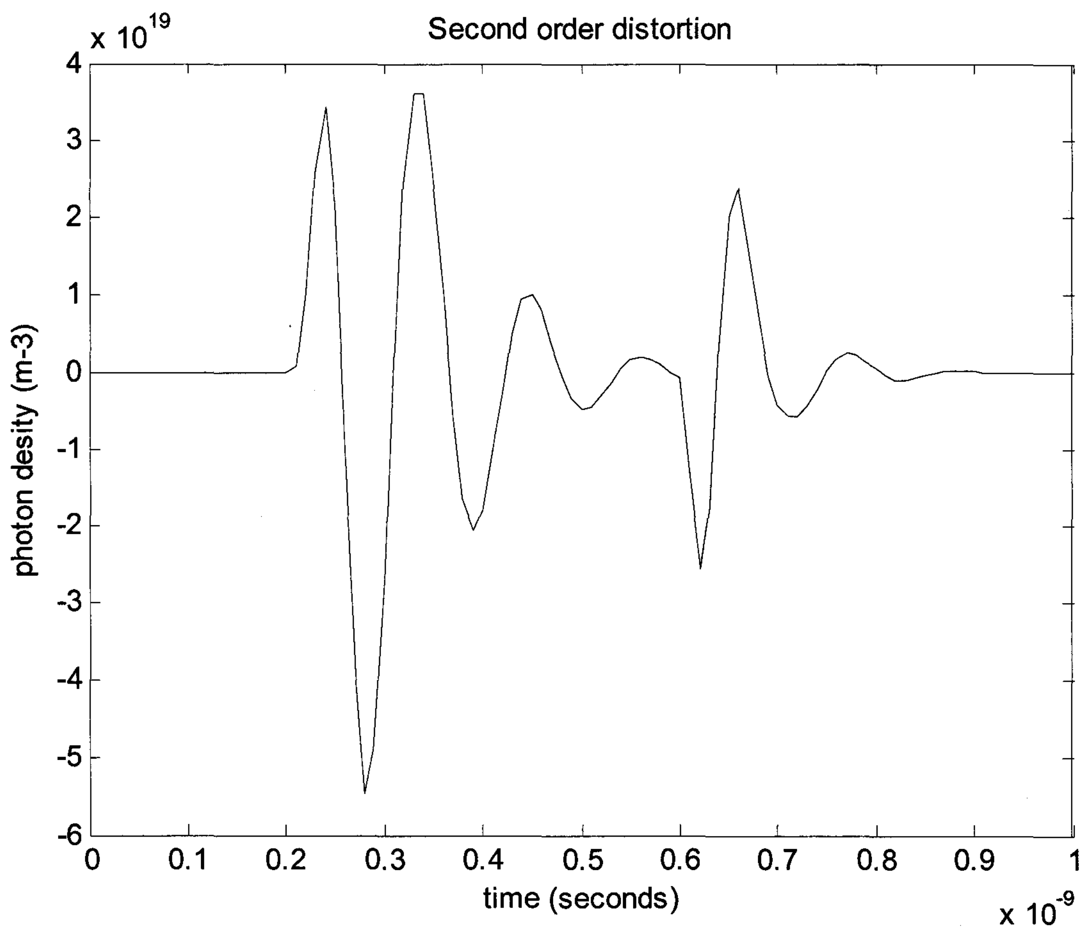

Figure 4.4: Second-order nonlinear distortion of the output pulse

Compare output signal described by the second-order Volterra model to the result of the numerical model:

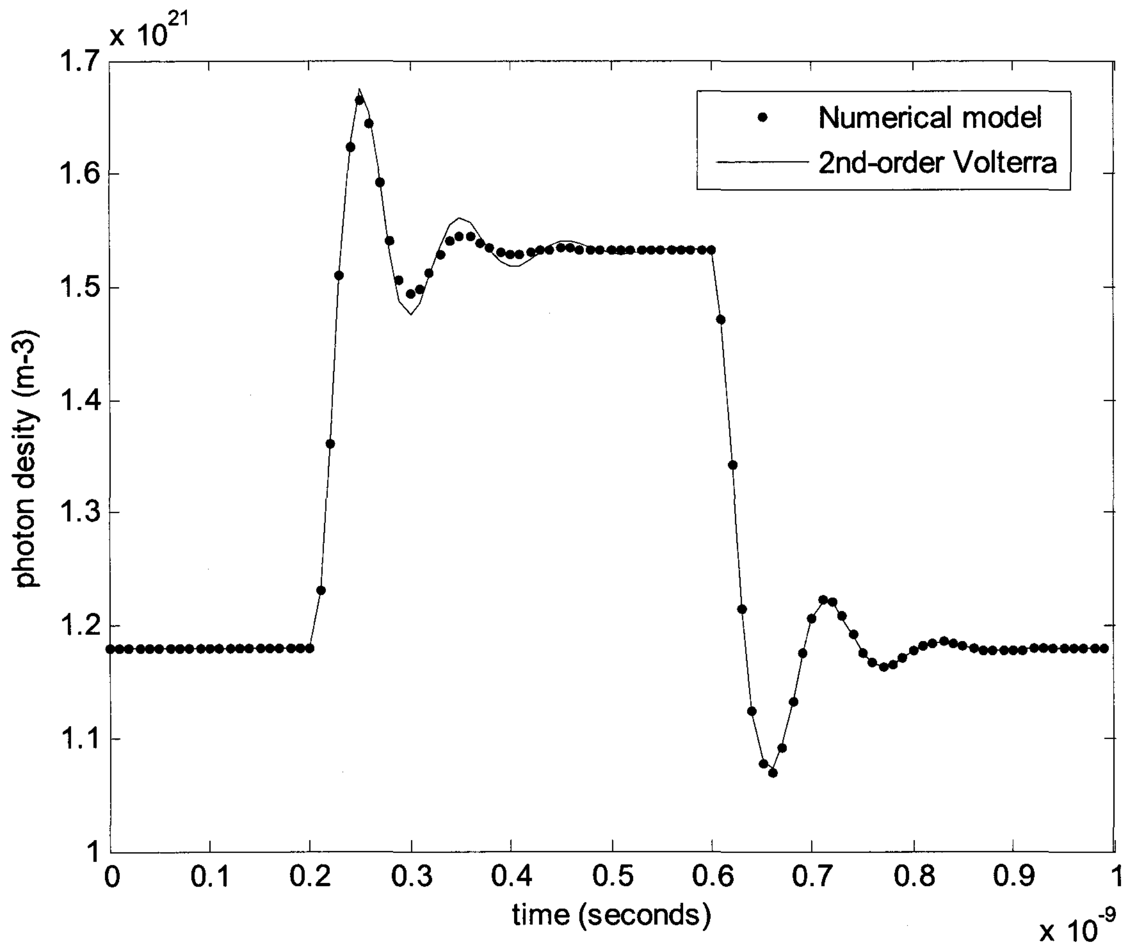

Figure 4.5: Output signal described by the second-order Volterra model

And we use the error function defined in the previous section 4.51 to show the improvement by the second-order Volterra model.

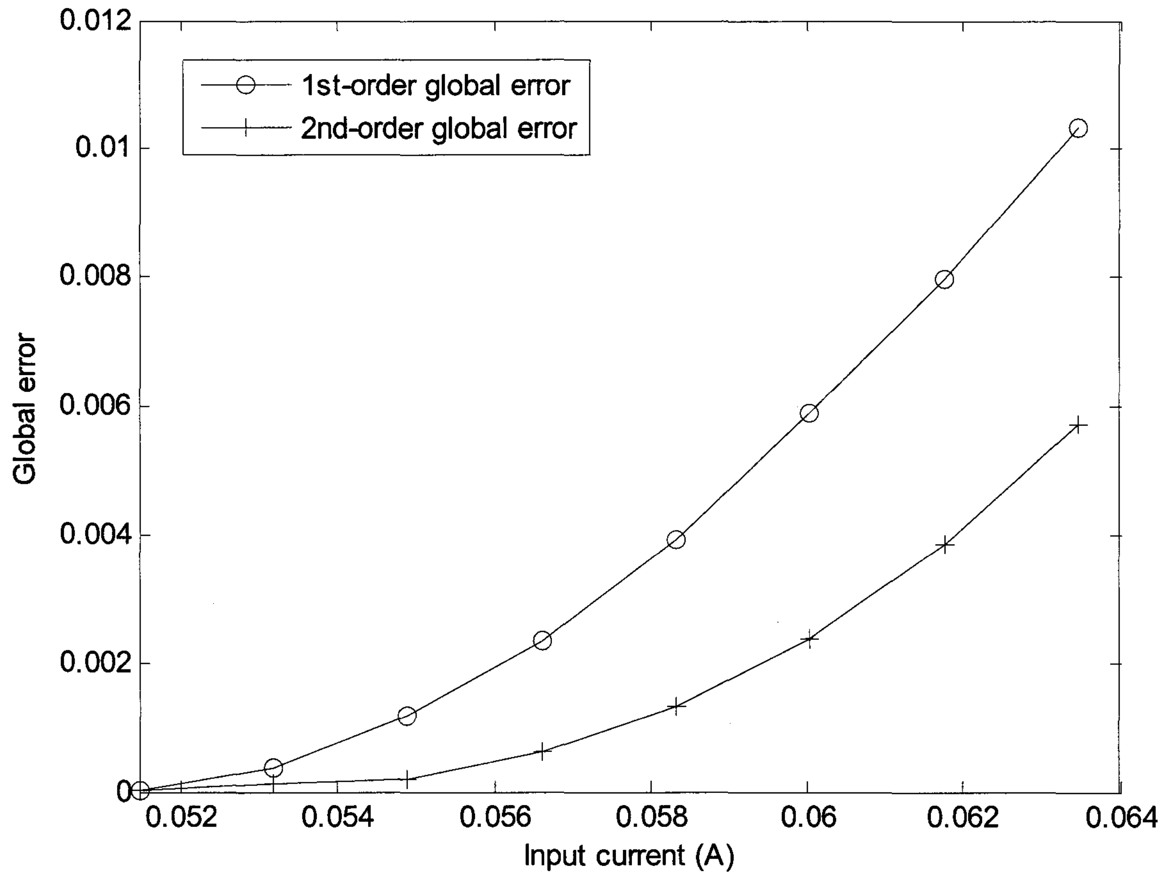

Figure 4.6: First-order and second-order errors comparison between the Volterra model and numerical model

4.7 Derivation of the Third-order Kernel of Rate Equations

In this section, we continue to derive the third-order Volterra kernel. A detailed procedure is provided in Appendix A. The result of the derivation is given below:

$$H_3(f_1, f_2, f_3) = \frac{\gamma\Gamma d}{c}(a - ((1-\varepsilon S_0)S_0 + \beta)) \quad (4.7.1)$$

$$G_3(f_1, f_2, f_3) = -\frac{d}{c}(\gamma\Gamma(N_0 - N_{tr})(1-2\varepsilon S_0) + b) \quad (4.7.2)$$

Where $a = j2\pi(f_1 + f_2 + f_3) + (1-\varepsilon S_0)S_0 + 1$ (4.7.3)

$$b = j2\pi(f_1 + f_2 + f_3) - \gamma(\Gamma(N_0 - N_{tr})(1-2\varepsilon S_0) - 1) \quad (4.7.4)$$

$$c = ab + \gamma\Gamma(N_0 - N_{tr})(1-2\varepsilon S_0)((1-\varepsilon S_0)S_0 + \beta) \quad (4.7.5)$$

$$\begin{aligned} d = & -\gamma\Gamma\frac{2}{3}(N_0 - N_{tr})\varepsilon(H_1(f_1)H_2(f_2,f_3) + H_1(f_2)H_2(f_1,f_3) + H_1(f_3)H_2(f_1,f_2)) \\ & +\gamma\Gamma\frac{1}{3}(1-2\varepsilon S_0)(G_1(f_1)H_2(f_2,f_3) + G_1(f_2)H_2(f_1,f_3) + G_1(f_3)H_2(f_1,f_2)) \\ & +\gamma\Gamma\frac{1}{3}(1-2\varepsilon S_0)(H_1(f_1)G_2(f_2,f_3) + H_1(f_2)G_2(f_1,f_3) + H_1(f_3)G_2(f_1,f_2)) \\ & -\gamma\Gamma\frac{1}{3}\varepsilon(H_1(f_1)H_1(f_2)G_1(f_3) + H_1(f_1)G_1(f_2)H_1(f_3) + G_1(f_1)H_1(f_2)H_1(f_3)) \end{aligned} \quad (4.7.6)$$

4.7.1 Simulation Result

Now we are calculating the third-order nonlinear distortion of the laser diode with the input signal amplitude $\Delta I = 0.6Ith$ on the bias current $I_b = 3Ith$. The third-order nonlinear distortion is in shown in Figure 4.7:

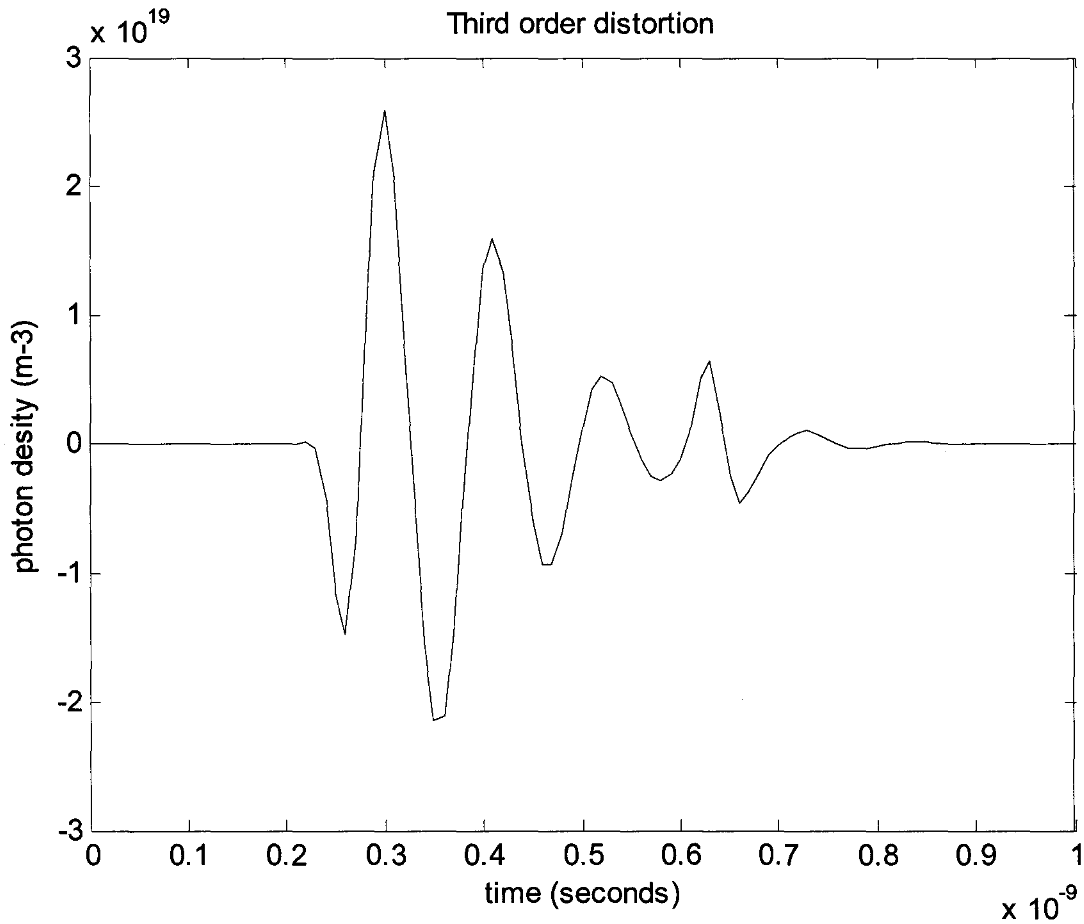

Figure 4.7: Third-order nonlinear distortion of the output pulse

The output signal described by the third-order Volterra model is in comparison with the result of the numerical model shown in Figure 4.8:

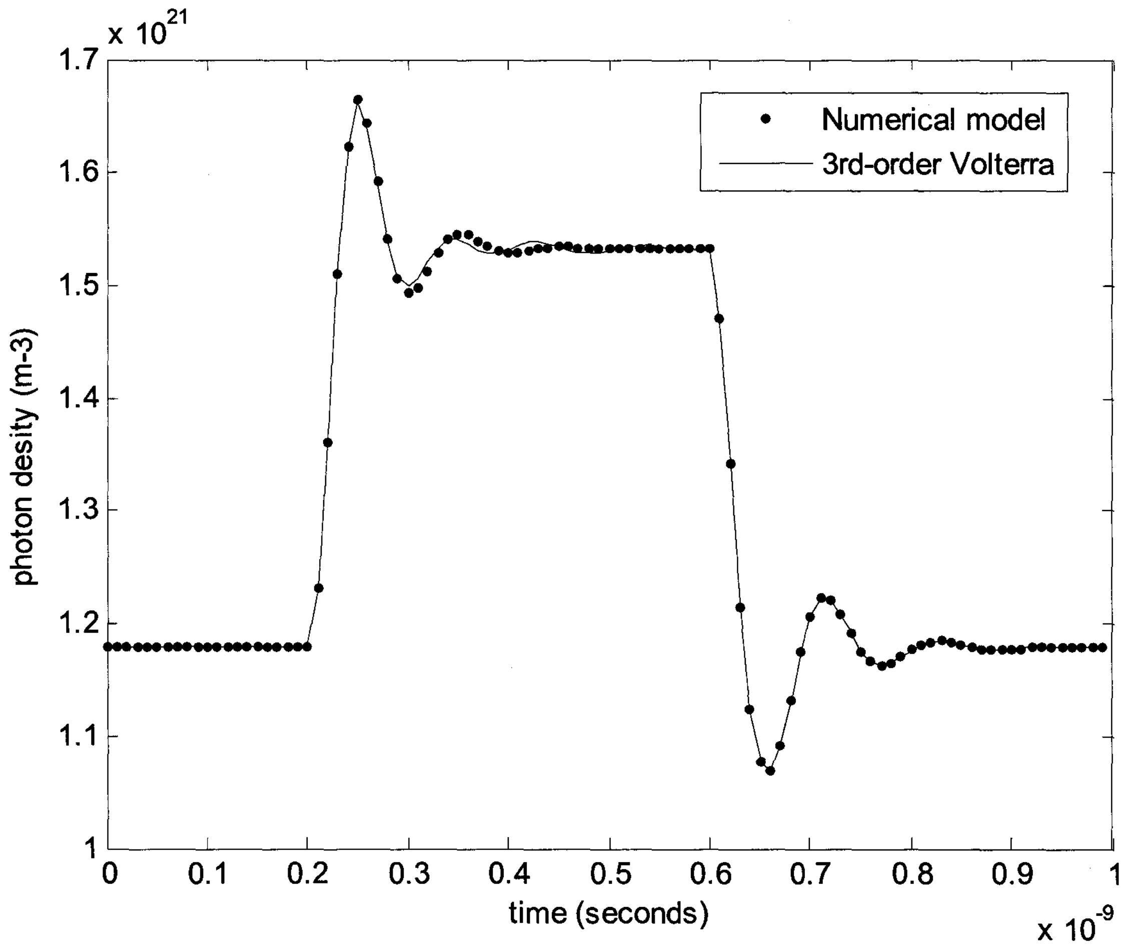

Figure 4.8: Output signal of the third-order Volterra model

It is obvious to see that the third-order Volterra model can describe the nonlinear distortion quite accurately. And we also plot the three level errors in Figure 4.9 below.

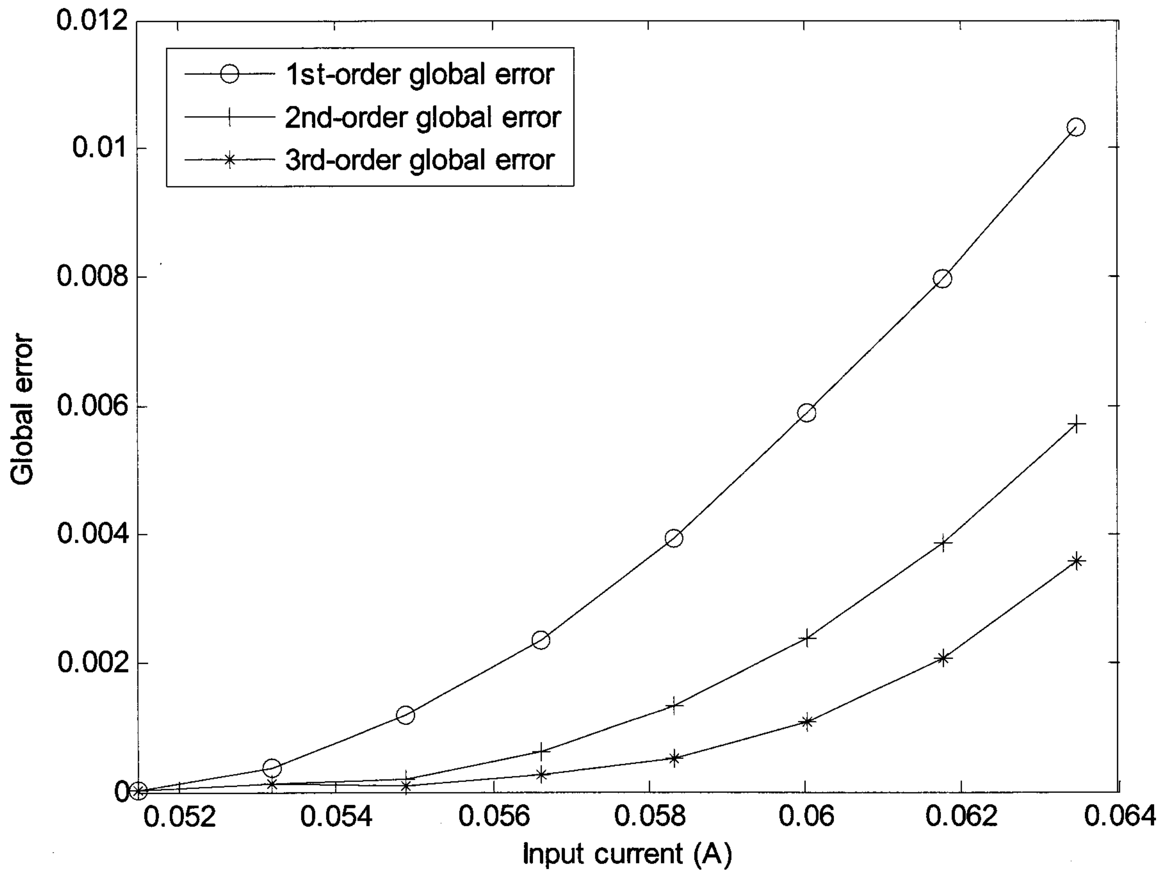

Figure 4.9: First-, second-, and third-order global errors comparisons

4.8 Conclusion

In this chapter, we discussed an analytical model based on the Volterra Series. The Volterra model has been applied to describe the modulation response of the laser diode in the first-, second-, and third-order separately. We found out that, the Volterra series model is a more general theoretical and actuarial model to analyze the nonlinearities of the laser diode.

Chapter 5
P^{th}-order Inverse Method

A Volterra model has been established to analyze the nonlinearities of the laser diode in the previous sections. Designing an equalizer for a Volterra system is also an important application to recover the original input signal from the output signal. There are several techniques to equalize Volterra systems, such as the p^{th}-order inverse [3] and fixed point equalizers [18]. In this chapter, the p^{th}-order inverse method has been discussed to compensate the laser's nonlinearity distortions.

5.1 Introduction of the P^{th}-order Inverse Theory

The nonlinear system can be presented by the Volterra series:

$$\begin{aligned} y(t) &= h_0 + \int_{-\infty}^{+\infty} h_1(\tau_1)x(t-\tau_1)d\tau_1 \\ &+ \int_{-\infty}^{+\infty}\int_{-\infty}^{+\infty} h_2(\tau_1,\tau_2)x(t-\tau_1)x(t-\tau_2)d\tau_1 d\tau_2 \\ &+ \ldots + \int_{-\infty}^{+\infty}\ldots\int_{-\infty}^{+\infty} h_n(\tau_1,\tau_2,\ldots\tau_n)x(t-\tau_1)x(t-\tau_2)\ldots x(t-\tau_n)d\tau_1 d\tau_2\ldots d\tau_n + \ldots. \end{aligned} \quad (5.1.1)$$

Let $H[\bullet]$ denote the n^{th}-order Volterra operator where:

$$H[x(t)] = \int_{-\infty}^{+\infty}\int_{-\infty}^{+\infty} h_n(\tau_1,\tau_2\ldots\tau_n)x(t-\tau_1)x(t-\tau_2)\ldots x(t-\tau_n)d\tau_1 d\tau_2\ldots d\tau_n \quad (5.1.2)$$

And $y(t) = H[x(t)] = \sum_{n=1}^{\infty} H_n[x(t)] = H_0 + H_1[x(t)] + \ldots + H_n[x(t)]$ (5.1.3)

Let $K[\bullet]$ denote the p^{th}-order inverse operator, and

$$K[y(t)] = K_0 + K_1[y(t)] + K_2[y(t)] + ...K_p[y(t)] \tag{5.1.4}$$

If we define $G[\bullet]$ is a system that $K[\bullet]$ cascaded with $H[\bullet]$. For the new system G:

$$G[x(t)] = K_p[H_n(x(t))] = G_1[x(t)] + G_2[x(t)] + ... + G_{p+1}[x(t)] + ... + G_{pn}[x(t)] \tag{5.1.5}$$

The inverse operator $K[\bullet]$ works in system G as the following principles:

$$G_1(x(t)) = x(t), \quad G_2[x(t)] = G_3[x(t)] = ... = G_p[x(t)] = 0 \tag{5.1.6}$$

In the next section, the pth-order inverse $K[\bullet]$ of the nonlinear system with a transfer function H will be discussed and represented in a specific form.

5.2 Representation of Pth-order Inverse Operator

Volterra series is a power series with memory. It means that if we give the input a gain factor m, then the output of the nth-order Volterra kernel will be increase m^n times by the definition of the Volterra series. Therefore, if $y(t) = H[x(t)]$, H is the Volterra system operator, the output of the same system with the input $mx(t)$ has the following forms:

$$y'(t) = H[mx(t)] = \sum_{n=1}^{+\infty} m^n H_n[x(t)] = \sum_{n=1}^{+\infty} m^n y_n(t) \tag{5.2.1}$$

And we can use this characteristic to determine the kernel of the pth-inverse operator [3].

Assume $r(t)$ is the response for the input $x(t)$ in the system G in which the pth-order inverse system K cascaded with the nth-order Volterra system H. Separately, in the nth-order Volterra system H $y(t)$ is the output for the input $x(t)$. For the pth-order inverse system K, $y(t)$ is the input and the corresponding output is $r(t)$.

Therefore, for the whole system G, we have:

$$r(t) = G[x(t)] = K[H(x(t)] \tag{5.2.2}$$

Let the input $x(t)$ has a gain factor m,

$$r(t) = G[cx(t)] = K[H[cx(t)]] = K[\sum_{i=1}^{N} c^i y(t)] = \sum_{j=1}^{p} K_j\left[\sum_{i=1}^{N} c^i y_i(t)\right] \tag{5.2.3}$$

Where K_j is defined as follows:

$$K_j[y_{i1}, y_{i2}...y_{ij}] = \int_{-\infty}^{+\infty}...\int_{-\infty}^{+\infty} k_j(\tau_1, \tau_2, ...\tau_j) y_{i1}(t-\tau_1)...y_{ij}(t-\tau_j) d\tau_1...d\tau_j \tag{5.2.4}$$

Therefore:

$$\begin{aligned}
K_j\left[\sum_{i=1}^{N} c^i y_i(t)\right] &= \int_{-\infty}^{+\infty}...\int_{-\infty}^{+\infty} k_j(\tau_1, \tau_2...\tau_j)\left[\sum_{i1=1}^{N} c^{i1} y_{i1}(t)\right]...\left[\sum_{ij=1}^{N} c^{ij} y_{ij}(t)\right] d\tau_1...d\tau_j \\
&= \int_{-\infty}^{+\infty}...\int_{-\infty}^{+\infty} k_j(\tau_1, \tau_2...\tau_j)\sum_{i1=1}^{N}...\sum_{ij=1}^{N} c^{i1}...c^{ij} y_{i1}(t)...y_{ij}(t) d\tau_1...d\tau_j \\
&= \sum_{i1=1}^{N}...\sum_{ij=1}^{N} c^{i1}...c^{ij} y_{i1}(t)...y_{ij}(t) K_j[y_{i1}(t), y_{i2}(t)...y_{ij}(t)]
\end{aligned} \tag{5.2.5}$$

and

$$r(t) = G[cx(t)] = \sum_{j=1}^{p}\left(\sum_{i1=1}^{N}...\sum_{ij=1}^{N} c^{i1}...c^{ij} y_{i1}(t)...y_{ij}(t) K_j[y_{i1}(t), y_{i2}(t)...y_{ij}(t)]\right) \tag{5.2.6}$$

We have defined system G in the previous section be a system that an nth-order Volterra system followed by a pth-order inverse system. So G must satisfy the following conditions:

$$G_1(cx(t)) = cx(t), \tag{5.2.7}$$

$$G_2[cx(t)] = c^2 G_2[x(t)] = 0, \tag{5.2.8}$$

$$G_3[cx(t)] = c^3 G_3[x(t)] = 0, \tag{5.2.9}$$

...

$$G_p[cx(t)] = c^p G_p[x(t)] = 0. \tag{5.2.10}$$

Now the operator $G_n[\bullet]$ can be expressed in terms of the Volterra operator $H_n[\bullet]$ and the inverse operator $K_p[\bullet]$ by means of locating the coefficients c^n.

For the first-order, the output of the system G has the coefficient c, according to the right hand of the equation (5.2.6) , we find out that if and only if $j=1$ and $i_1 = 1$, we can obtain the first-order operator by equating the two components having the first power of c and follow the constrain condition (5.2.7). Finally, we have:

$$G_1[x(t)] = K_1[y_1(t)] = K_1[H_1[x(t)]] = K_1 H_1[x(t)] = x(t) \tag{5.2.11}$$

Therefore, $K_1 H_1 = I$ and we get the first-order inverse operator K_1 in the forms of $H_1 : K_1 = \frac{1}{H_1}$ the same as the linear model inverse discussed in chapter 3.

The second-order inverse operator can be obtained in the same procedure as the first-order inverse operator derivation. Through observation on the equations(5.2.6), we find out that we can obtain the coefficients c^2 by letting $j = 1, i_1 = 2$ and $j = 2, i_1 = i_2 = 1$, equating the components with coefficients c^2 and constrained by the condition(5.2.8), we obtain:

$$G_2[x] = K_1[y_2] + K_2[y_1] = K_1[H_2[x(t)]] + K_2[H_1[x(t)]] = 0 \quad (5.2.12)$$

$$K_1 H_2 = -K_2 H_1 \quad (5.2.13)$$

$$K_2 = -K_1 H_2 H_1^{-1} = -K_1 H_2 K_1 \quad (5.2.14)$$

Therefore, we get the second-order operator $K_2[\bullet]$ in terms of the first- and second-order Volterra operator $H_1[\bullet], H_2[\bullet]$ and the first-order inverse $K_1[\bullet]$.

Repeating the above procedure to obtain the third-order inverse operator, we obtain:

$$G_3[x(t)] = K_1[y_3] + K_2[y_2, y_1] + K_2[y_1, y_2] + K_3[y_1] \quad (5.2.15)$$

According to the representation of $K_j[y_{i1}, y_{i2} \ldots y_{ij}]$:

$$K_j[y_{i1}, y_{i2} \ldots y_{ij}] = \int_{-\infty}^{+\infty} \ldots \int_{-\infty}^{+\infty} k_j(\tau_1, \tau_2, \ldots \tau_j) y_{i1}(t-\tau_1) \ldots y_{ij}(t-\tau_j) d\tau_1 \ldots d\tau_j \quad (5.2.16)$$

And suppose $k_j(\tau_1, \tau_2, \ldots \tau_j)$ be symmetric.

$$\begin{aligned} K_2[y_2, y_1] = K_2[y_1, y_2] &= \int_{-\infty}^{+\infty} \int_{-\infty}^{+\infty} k_2(\tau_1, \tau_2) y_1(t-\tau_1) y_2(t-\tau_2) d\tau_1 d\tau_2 \\ &= \frac{1}{2} \int_{-\infty}^{+\infty} \int_{-\infty}^{+\infty} k_2(\tau_1, \tau_2)[(y_1(t-\tau_1) + y_2(t-\tau_2))^2 - y_1^2(t-\tau_1) - y_2^2(t-\tau_2)] d\tau_1 d\tau_2 \\ &= \frac{1}{2}(K_2[y_1 + y_2] - K_2[y_1] - K_2[y_2]) \end{aligned} \quad (5.2.17)$$

So $G_3[x(t)] = K_1[y_3] + K_2[y_1 + y_2] - K_2[y_1] - K_2[y_2] + K_3[y_1]$ (5.2.18)

Applying the constrained condition $G_3[x(t)] = 0$, so that:

$$K_3[H_1[x(t)]] = -K_1[H_3[x(t)]] - K_2[H_1[x(t)] + H_2[x(t)]] + K_2[H_1[x(t)]] + K_2[H_2[x(t)]] \quad (5.2.19)$$

Therefore, the third-order inverse operation is obtained:

$$K_3 = -K_1 H_3 K_1 - K_2[H_1 + H_2] K_1 + K_2 H_1 K_1 + K_2 H_2 K_1 \quad (5.2.20)$$

The procedure can be repeated until we have derived the pth-order inverse operator $K_p[\bullet]$. And we get the conclusion that the pth-order inverse operator can be expressed in terms of the Volterra operator $H_1, H_2 ... H_p$ and the inverse operator $K_1, K_2 ... K_{p-1}$.

5.3 Design the Third-order Inverse Model of the Laser Diode

Next we will design a third-order inverse system to compensate the nonlinear distortion of the laser diode. First we define H_1, H_2, H_3 are the nonlinear transfer functions of the laser diode, K_1, K_2, K_3 are the transfer functions of the nonlinear distortion compensation system and G is the overall system that K cascaded with H. The ideal output of the overall system G with a rectangular input pulse should also be a rectangular pulse without nonlinear distortions. If the overall system G satisfies the ideal situation, we have the following constrain conditions up to the third order:

$$G_1(x(t)) = H_1(0)x(t), \tag{5.3.1}$$

$$G_2[x(t)] = G_3[x(t)] = 0, \tag{5.3.2}$$

The first-, second-, and third-order inverse operators are obtained separately as follows:

$$G_1[x(t)] = K_1[y_1(t)] == K_1 H_1[x(t)] = H_1(0)x(t) \tag{5.3.3}$$

The first-order inverse transfer function is:

$$K_1 = H_1(0)H_1. \tag{5.3.4}$$

As for the second order transfer function, we have the relationship:

$$G_2[x] = K_1[y_2] + K_2[y_1] = K_1[H_2[x(t)]] + K_2[H_1[x(t)]] = 0 \tag{5.3.5}$$

Therefore the second-order inverse transfer function is obtained:

$$K_2 = -K_1 H_2 H_1^{-1} \tag{5.3.6}$$

Repeat the same procedure on the third-order relationships:

$$K_3[H_1[x(t)]] = -K_1[H_3[x(t)]] - K_2[H_1[x(t)] + H_2[x(t)]] + K_2[H_1[x(t)]] + K_2[H_2[x(t)]] \tag{5.3.7}$$

Finally we get the third-order transfer function of the nonlinear compensation system:

$$K_3 = -K_1 H_3 H_1^{-1} - K_2[H_1 + H_2]H_1^{-1} + K_2 H_1 H_1^{-1} + K_2 H_2 H_1^{-1} \tag{5.3.8}$$

5.3.1 Simulation Result

We test the third-order compensation scheme performance by the follow steps. First let a rectangular pulse with modulated current amplitude $\Delta I = 0.6Ith$ biased on $I_b = 3Ith$ be the input of the third-order Volterra system. Then let the output of the Volterra model be the input of the nonlinear compensation system G to simulate the reshaped output signal.

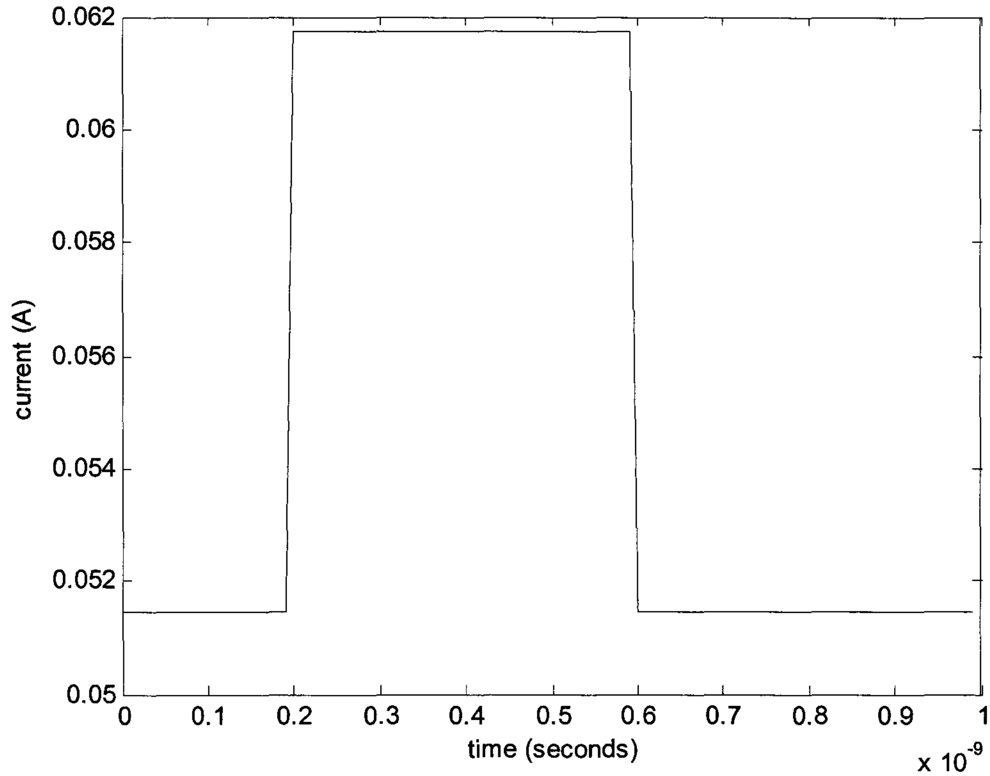

Figure 5.1: Input rectangular pulse with amplitude 10.3 mA of the bias current 51.5mA.

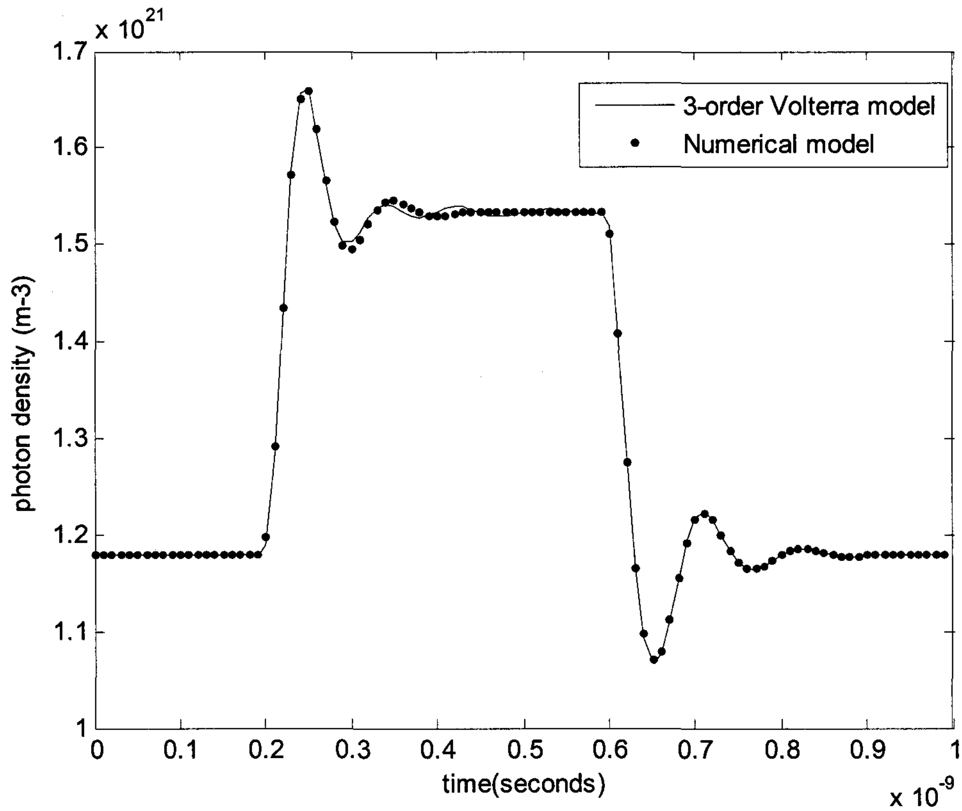

Figure 5.2: Output signal of the third-order Volterra model

In this section simulation, we test the inverse operators derived in section 5.3 on the third-order Volterra model and the numerical model separately. Figure 5.3, Figure 5.4, Figure 5.5 shows the compensation result based on the first-, second-, and third-order inverse operator for the third-order Volterra model respectively.

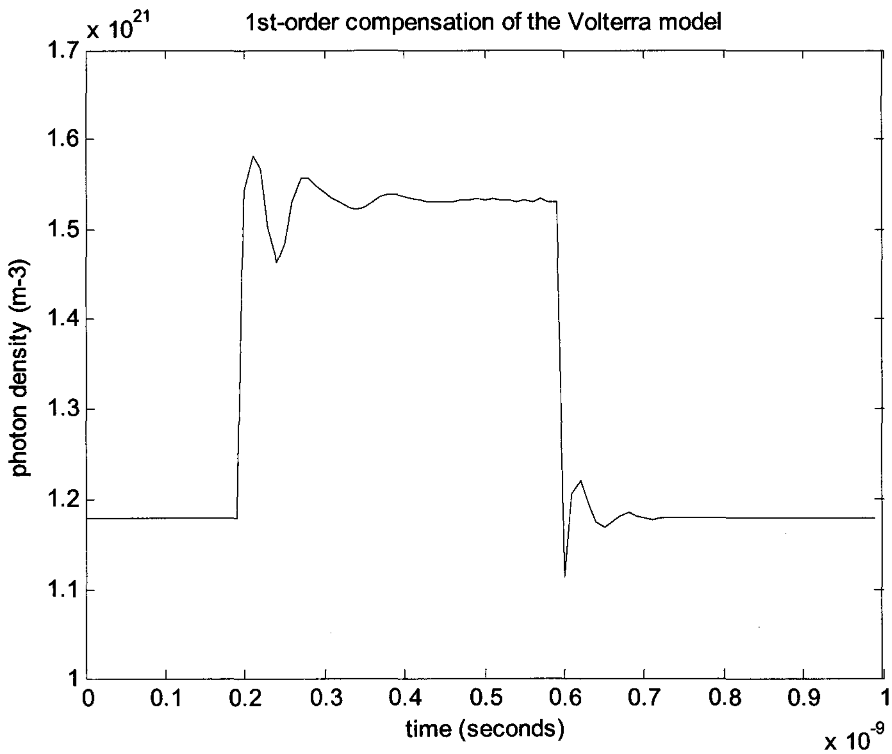

Figure 5.3: First-order compensation of the third-order Volterra model

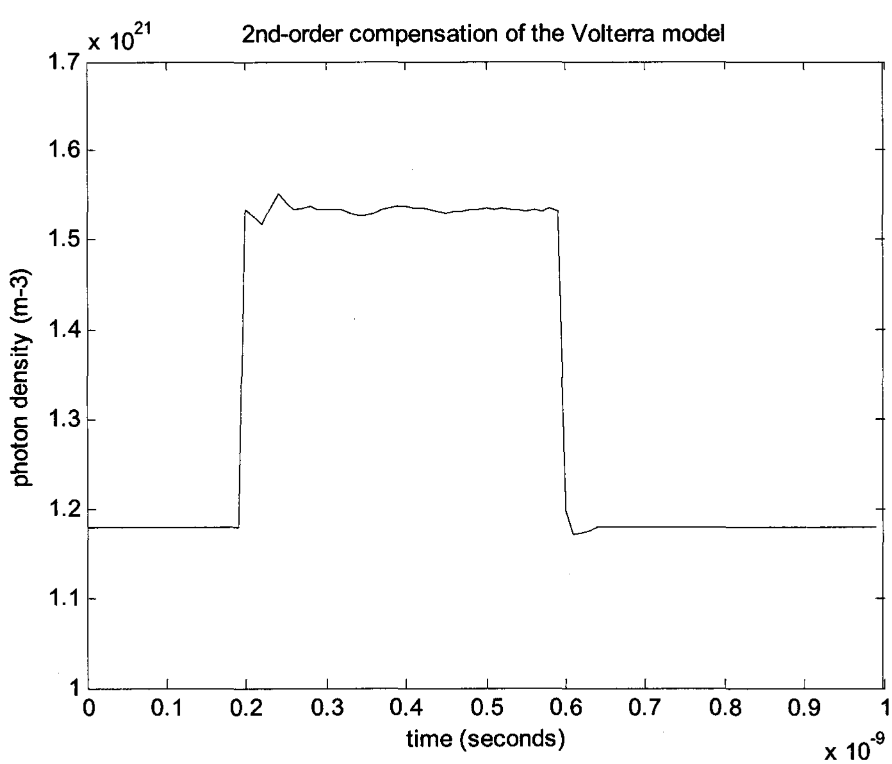

Figure 5.4: Second-order compensation of the third-order Volterra model

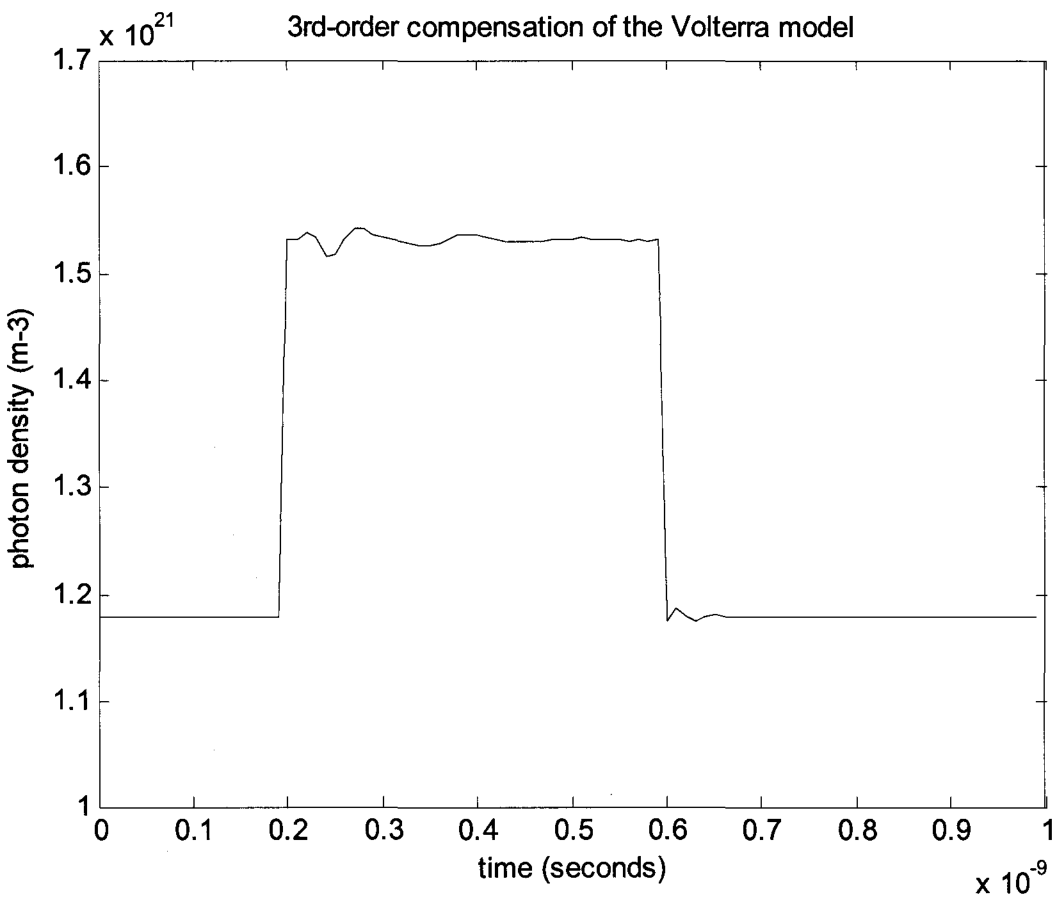

Figure 5.5: Third-order compensation of the third-order Volterra model

Next, let the nonlinear compensation system connect to the numerical model. The compensation system performance is also explored in the first-, second-, and third-order respectively.

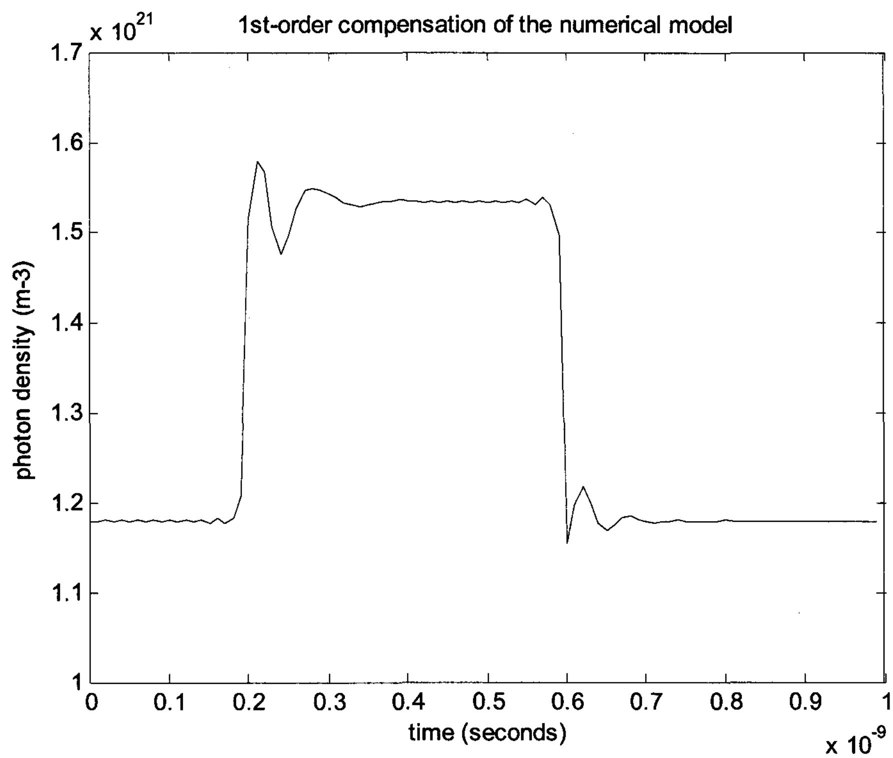

Figure 5.6: First-order compensation of the numerical model

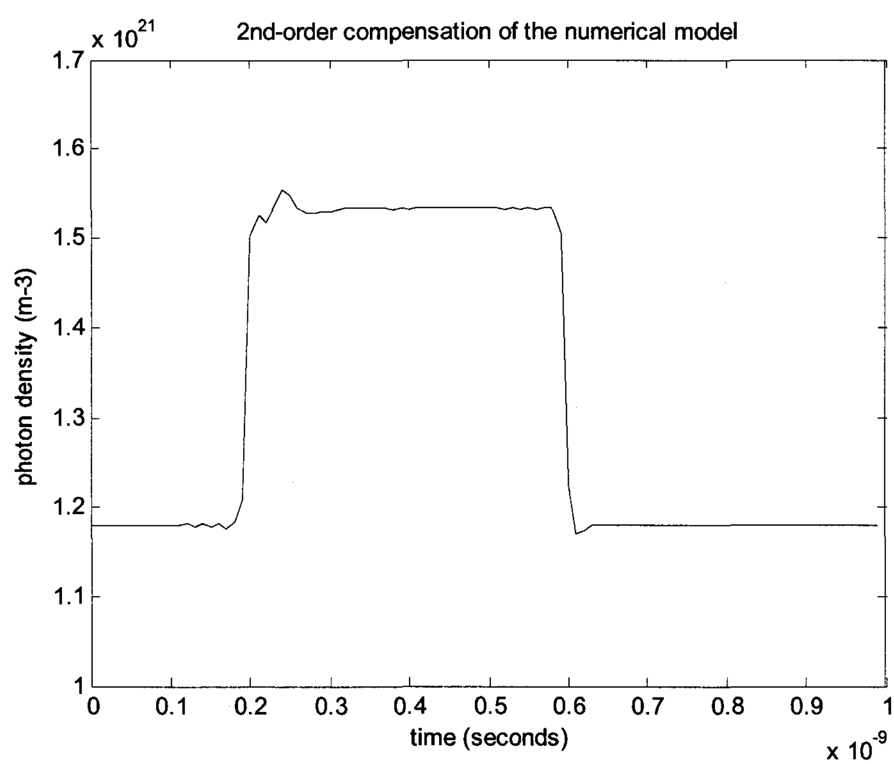

Figure 5.7: Second-order compensation of the numerical model

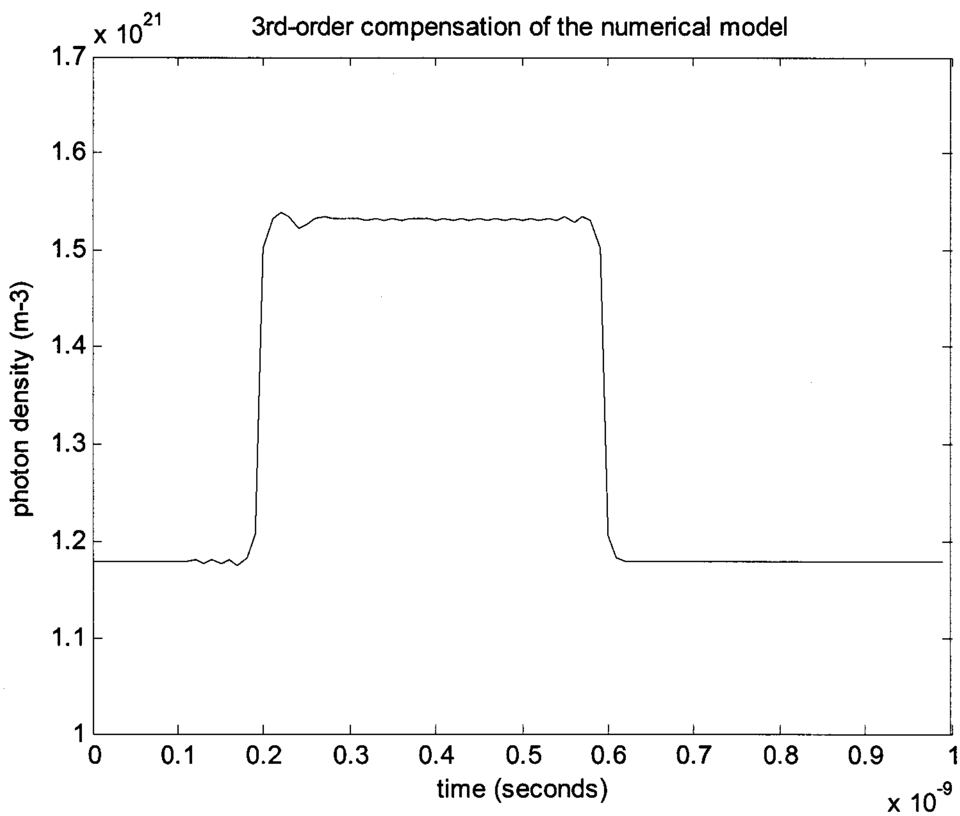

Figure 5.8: Third-order compensation of the numerical model

Here we use the global error function defined in section 4.5.1 to describe the discrepancy between reshaped output signal and the ideal rectangular pulse to show 'how much' the nonlinear distortion has been compensated. Figure 5.9 and Figure 5.10 shows the compensation ability of the inverse scheme for the third-order Volterra model and the numerical model with different modulated current amplitude on the bias current 51.5mA.

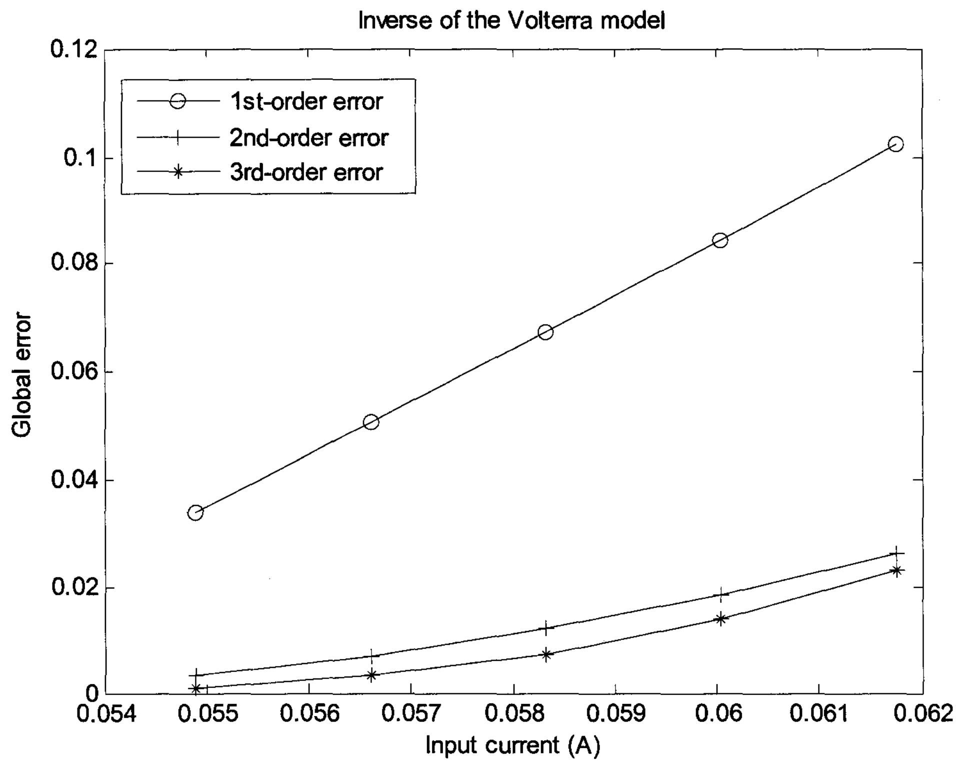

Figure 5.9: Comparison of compensation errors in Volterra model

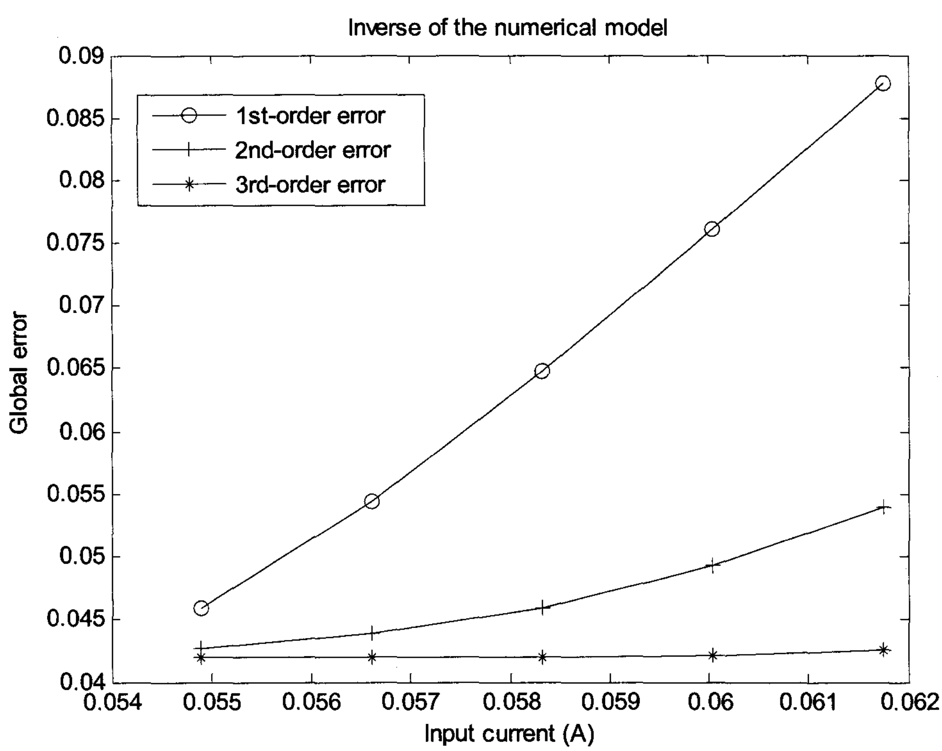

Figure 5.10: Comparison of compensation errors in numerical model

5.4 Conclusion

In this chapter, the theory of p^{th}-order inverse of a Volterra system has been discussed and applied. We derived nonlinear inverse operator up to the third-order for the nonlinear rate equation system using the p^{th}-order inverse theory. A simulation is conducted to show the compensation effect for third-order Volterra model and numerical model respectively.

Chapter 6
Conclusion

6.1 Conclusion

In the thesis, we use an analytical model based on the Volterra Series to analyze the nonlinearity of the laser diode. Through the comparison to the small signal model, we find out that Volterra series model is a more general analytical model and can describe the response of the directly modulated laser diode accurately. Then the p^{th}-order Inverse theory is applied to compensate the nonlinear distortions in the laser diode. By simulating the compensation scheme, we found out that the compensation system can cancel the most nonlinear distortion when the laser diode is operated on a fixed bias current.

Appendix E

Derivation of Third-order Transfer Function

This appendix gives details of the derivation of the third-order Volterra kernel as discussed in Chapter 4, subsection 7. The procedure is similar with the first- and second-order derivations with the sum of three exponentials as the input $I(t) = \exp(j2\pi f_1 t) + \exp(j2\pi f_2 t) + \exp(j2\pi f_3 t)$, according to(4.3.5), we obtain the following equations:

$$
\begin{aligned}
N(t) &= G_1(f_1)\exp(j2\pi f_1 t) + G_1(f_2)\exp(j2\pi f_2 t) + G_1(f_3)\exp(j2\pi f_3 t) \\
&+2G_2(f_1,f_2)\exp(j2\pi(f_1+f_2)t)+2G_2(f_1,f_3)\exp(j2\pi(f_1+f_3)t)+2G_2(f_2,f_3)\exp(j2\pi(f_2+f_3)t) \\
&+G_2(f_1,f_1)\exp(j4\pi f_1 t)+G_2(f_2,f_2)\exp(j4\pi f_2 t)+G_2(f_3,f_3)\exp(j4\pi f_3 t) \\
&+3!G(f_1,f_2,f_3)\exp(j2\pi(f_1+f_2+f_3))+\frac{3!}{1!2!}G(f_1,f_1,f_2)\exp(j2\pi(f_1+f_2+f_3)) \\
&+\frac{3!}{1!2!}G(f_1,f_2,f_2)\exp(j2\pi(f_1+2f_2))+\frac{3!}{1!2!}G(f_1,f_1,f_3)\exp(j2\pi(2f_1+f_3)) \\
&+\frac{3!}{1!2!}G(f_1,f_3,f_3)\exp(j2\pi(f_1+2f_3))+\frac{3!}{1!2!}G(f_2,f_2,f_3)\exp(j2\pi(2f_2+f_3))+\frac{3!}{1!2!}G(f_2,f_3,f_3)\exp(j2\pi(f_2+2f_3)) \\
&+G(f_1,f_1,f_1)\exp(j6\pi f_1)+G(f_2,f_2,f_2)\exp(j6\pi f_2)+G(f_3,f_3,f_3)\exp(j6\pi f_3)
\end{aligned}
\tag{A.1}
$$

and

$$
\begin{aligned}
S(t) &= H_1(f_1)\exp(j2\pi f_1 t) + H_1(f_2)\exp(j2\pi f_2 t) + H_1(f_3)\exp(j2\pi f_3 t) \\
&+2H_2(f_1,f_2)\exp(j2\pi(f_1+f_2)t)+2H_2(f_1,f_3)\exp(j2\pi(f_1+f_3)t)+2H_2(f_2,f_3)\exp(j2\pi(f_2+f_3)t) \\
&+H_2(f_1,f_1)\exp(j4\pi f_1 t)+H_2(f_2,f_2)\exp(j4\pi f_2 t)+H_2(f_3,f_3)\exp(j4\pi f_3 t) \\
&+3!H(f_1,f_2,f_3)\exp(j2\pi(f_1+f_2+f_3))+\frac{3!}{1!2!}H(f_1,f_1,f_2)\exp(j2\pi(f_1+f_2+f_3))
\end{aligned}
$$

$$+\frac{3!}{1!2!}H(f_1,f_2,f_2)\exp(j2\pi(f_1+2f_2))+\frac{3!}{1!2!}H(f_1,f_1,f_3)\exp(j2\pi(2f_1+f_3))$$
$$+\frac{3!}{1!2!}H(f_1,f_3,f_3)\exp(j2\pi(f_1+2f_3))+\frac{3!}{1!2!}H(f_2,f_2,f_3)\exp(j2\pi(2f_2+f_3))+\frac{3!}{1!2!}H(f_2,f_3,f_3)\exp(j2\pi(f_2+2f_3))$$
$$+H(f_1,f_1,f_1)\exp(j6\pi f_1)+H(f_2,f_2,f_2)\exp(j6\pi f_2)+H(f_3,f_3,f_3)\exp(j6\pi f_3)$$

(A.2)

Finding out all the terms with the coefficients $3!\exp(j2\pi(f_1+f_2+f_3)t)$, then the third-order transfer function is determined by:

$$(j2\pi(f_1+f_2+f_3)+(1-\varepsilon S_0)S_0+1)G_3(f_1,f_2,f_3)$$
$$=-(N_0-N_{tr})(1-2\varepsilon S_0)G_3(f_1,f_2,f_3)$$
$$+\frac{2}{3}(N_0-N_{tr})\varepsilon(H_1(f_1)H_2(f_2,f_3)+H_1(f_2)H_2(f_1,f_3)+H_1(f_3)H_2(f_1,f_2))$$
$$-\frac{1}{3}(1-2\varepsilon S_0)(G_1(f_1)H_2(f_2,f_3)+G_1(f_2)H_2(f_1,f_3)+G_1(f_3)H_2(f_1,f_2))$$
$$-\frac{1}{3}(1-2\varepsilon S_0)(H_1(f_1)G_2(f_2,f_3)+H_1(f_2)G_2(f_1,f_3)+H_1(f_3)G_2(f_1,f_2))$$
$$+\frac{1}{3}\varepsilon(H_1(f_1)H_1(f_2)G_1(f_3)+H_1(f_1)G_1(f_2)H_1(f_3)+G_1(f_1)H_1(f_2)H_1(f_3))$$

(A.3)

and

$$(j2\pi(f_1+f_2+f_3)-\gamma(\Gamma(N_0-N_{tr})(1-2\varepsilon S_0)-1)H_3(f_1,f_2,f_3)$$
$$=-\gamma\Gamma(\beta+(1-\varepsilon S_0)S_0)G_3(f_1,f_2,f_3)$$
$$-\gamma\Gamma\frac{2}{3}(N_0-N_{tr})\varepsilon(H_1(f_1)H_2(f_2,f_3)+H_1(f_2)H_2(f_1,f_3)+H_1(f_3)H_2(f_1,f_2))$$
$$+\gamma\Gamma\frac{1}{3}(1-2\varepsilon S_0)(G_1(f_1)H_2(f_2,f_3)+G_1(f_2)H_2(f_1,f_3)+G_1(f_3)H_2(f_1,f_2))$$
$$+\gamma\Gamma\frac{1}{3}(1-2\varepsilon S_0)(H_1(f_1)G_2(f_2,f_3)+H_1(f_2)G_2(f_1,f_3)+H_1(f_3)G_2(f_1,f_2))$$
$$-\gamma\Gamma\frac{1}{3}\varepsilon(H_1(f_1)H_1(f_2)G_1(f_3)+H_1(f_1)G_1(f_2)H_1(f_3)+G_1(f_1)H_1(f_2)H_1(f_3))$$

(A.4)

Let $a = j2\pi(f_1 + f_2 + f_3) + (1 - \varepsilon S_0)S_0 + 1$ (A.5)

$$b = j2\pi(f_1 + f_2 + f_3) - \gamma(\Gamma(N_0 - N_{tr})(1 - 2\varepsilon S_0) - 1) \quad \text{(A.6)}$$

$$c = ab + \gamma\Gamma(N_0 - N_{tr})(1 - 2\varepsilon S_0)((1 - \varepsilon S_0)S_0 + \beta) \quad \text{(A.7)}$$

$$\begin{aligned} d = &-\gamma\Gamma\frac{2}{3}(N_0 - N_{tr})\varepsilon(H_1(f_1)H_2(f_2,f_3) + H_1(f_2)H_2(f_1,f_3) + H_1(f_3)H_2(f_1,f_2)) \\ &+\gamma\Gamma\frac{1}{3}(1 - 2\varepsilon S_0)(G_1(f_1)H_2(f_2,f_3) + G_1(f_2)H_2(f_1,f_3) + G_1(f_3)H_2(f_1,f_2)) \\ &+\gamma\Gamma\frac{1}{3}(1 - 2\varepsilon S_0)(H_1(f_1)G_2(f_2,f_3) + H_1(f_2)G_2(f_1,f_3) + H_1(f_3)G_2(f_1,f_2)) \\ &-\gamma\Gamma\frac{1}{3}\varepsilon(H_1(f_1)H_1(f_2)G_1(f_3) + H_1(f_1)G_1(f_2)H_1(f_3) + G_1(f_1)H_1(f_2)H_1(f_3)) \end{aligned}$$

(A.8)

Finally, the third-order transfer function of rate equation has been derived:

$$H_3(f_1,f_2,f_3) = \frac{\gamma\Gamma d}{c}(a - ((1 - \varepsilon S_0)S_0 + \beta)) \quad \text{(A.9)}$$

$$G_3(f_1,f_2,f_3) = -\frac{d}{c}(\gamma\Gamma(N_0 - N_{tr})(1 - 2\varepsilon S_0) + b) \quad \text{(A.10)}$$

Bibliography

[1] Kressel, H., and Butler, J.K., Semiconductor Lasers and Heterojunction LED's. New York: Academic, 1977.

[2] H. M. Salgado and J.J. O'Reilly, Volterra Series Analysis of Distortion in Semiconductor Laser Diodes, Proc. Inst. ELec. Eng. J, vol. 138, pp. 379-382, Dec. 1991.

[3] M. Schetzen, Theory of pth-Order Inverse of Nonlinear Systems, IEEE Trans. Circuits Syst., vol. cas-23, pp. 285-291, May 1976.

[4] L. Hassine, Z. Toffano, F. Lamnabhi-Lagarrigue, A. Destrez, and C. Birocheau, Volterra Functional Series Expansions for Semiconductor Lasers under Modulation, IEEE J. Quantum Electron., 30, 918-928, 1994.

[5] R. S. Vodhanel, A. F. Elrefaie, R. E. Wagner, M. Z. Iqbal, J. L. Gimlett, and S. Tsuji, 10-to-20 gbit/s modulation performance of 1.5μm distributed feedback lasers for frequency-shift-keying systems, J. Lightwave Technol., vol. 7, pp. 1454-1460, Oct. 1989.

[6] M. Schetzen, Measurement of the Kernels of a Non-linear System of Finite Order, Int. J. of Control, vol. 1, pp. 251-263, Mar, 1965.

[7] T. Schaer, R. Rusnov, S. Eagle, J. Jastrebski, S. Albanese, and X. Fernando, "A dynamic simulation model for semiconductor laser diodes", IEEE CCECE 2003, vol. 1, pp. 293-297, 2003

[8] J.J. Bussgang, L. Ehrman, J. W. Graham, Analysis of nonlinear systems with multiple inputs, Proceedings of the IEEE , vol.62, no.8, pp. 1088-1119, Aug. 1974.

[9] Z. Gajic, Linear Dynamic Systems and Signals, 1st ed., Prentice Hall, 2003.

[10] S. Haykin, and B. V. Veen, Signals and Systems, 2nd ed., John Wiley & Sons, Inc., 2005.

[11] G. P. Agrawal, Fiber-Optic Communication Systems, New York: Wiley, 2002.

[12] G. P. Agrawal, and N. K. Dutta, Semiconductor Lasers, 2nd ed, New York: Van Nostrand Reinhold, 1993

[13] R.S. Tucker, and I. P. Kaminow, High-Frequency Characteristics of Directly Modulated InGaAsP Ridge Waveguide and Buried Heterostructures, J. Lightwave Technol., vol.2, no.4, pp. 385-393, Aug 1984.

[14] W. J. Rugh, Nonlinear System Theory: The Volterra / Wiener Approach, Baltimore: The Johns Hopkins University Press, 1981.

[15] J. Tsimbinos, Identification and Compensation of Nonlinear Distortion, Ph.D. Thesis, University of South Australia, 1995.

[16] J. A. Cherry, Distortion analysis of weakly nonlinear filters using Volterra series, M.Eng. Thesis, Carleton Univ., Ottawa, Ont., Canada, 1994.

[17] L. Illing and M.B. Kennel, Shaping current waveforms for direct modulation of semiconductor lasers, Quantum Electronics, IEEE Journal of, vol. 40, no.5,

pp.445-452, May 2004.

[18] R. D. Nowak and B. D. Van Veen, Volterra filter equalization: A fixed point approach, IEEE trans. Signal Processing, vol. 44, pp. 377-388, 1997.

[19] A. J. Redfern and G. T. Zhou, A root method for Volterra system equalization, IEEE Signal Processing Lett., vol. 5, pp. 285-288, Nov. 1998.

[20] L. Bjerkan, A. Royset, L. Hafskjaer, and D. Myhre, Measurement of Laser Parameters for Simulation of High-Speed Fiberoptic Systems, Journal of Lightwave Technology, vol. 14, No.5, pp. 839-850, May 1996